molecular pharmaceutics

Article

pubs.acs.org/molecularpharmaceutics

Enhanced Oral Absorption of Hydrophobic and Hydrophilic Drugs Using Quaternary Ammonium Palmitoyl Glycol Chitosan Nanoparticles

Adeline Siew,[†] Hang Le,[†] Marion Thiovolet,[†] Paul Gellert,[§] Andreas Schatzlein,[‡] and Ijeoma Uchegbu*[,†]

[†]Department of Pharmaceutics, School of Pharmacy and [‡]Department of Biological and Physical Chemistry, School of Pharmacy, University of London, 29−39 Brunswick Square, London WC1N 1AX, U.K.

[§]Astra Zeneca, Mereside Alderly Park, Macclesfield, Cheshire, SK10 4TG, U.K.

Supporting Information

ABSTRACT: As 95% of all prescriptions are for orally administered drugs, the issue of oral absorption is central to the development of pharmaceuticals. Oral absorption is limited by a high molecular weight (>500 Da), a high log *P* value (>2.0) and low gastrointestinal permeability. We have designed a triple action nanomedicine from a chitosan amphiphile: quaternary ammonium palmitoyl glycol chitosan (GCPQ), which significantly enhances the oral absorption of hydrophobic drugs (e.g., griseofulvin and cyclosporin A) and, to a lesser extent, the absorption of hydrophilic drugs (e.g., ranitidine). The griseofulvin and cyclosporin A C_{max} was increased 6- and 5-fold respectively with this new nanomedicine. Hydrophobic drug absorption is facilitated by the nanomedicine: (a) increasing the dissolution rate of hydrophobic molecules, (b) adhering to and penetrating the mucus layer and thus enabling intimate contact between the drug and the gastrointestinal epithelium absorptive cells, and (c) enhancing the transcellular transport of hydrophobic compounds. Although the C_{max} of ranitidine was enhanced by 80% with the nanomedicine, there was no appreciable opening of tight junctions by the polymer particles.

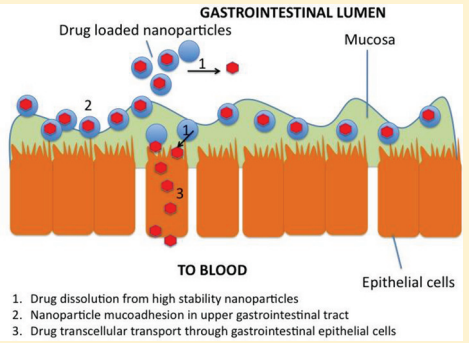

KEYWORDS: *oral absorption, chitosan amphiphiles, hydrophobic drugs, hydrophilic drugs, mucoadhesion, transcellular transport, griseofulvin, cyclosporin A, idarubicin, ranitidine*

INTRODUCTION

The oral route is the most popular choice for drug delivery as it offers good patient compliance due to its acceptability, convenience and ease of administration. The avoidance of pain and discomfort associated with injections and the elimination of possible infections caused by inappropriate use or reuse of needles make the oral route especially relevant for the treatment of pediatric and geriatric patients, particularly when therapies are administered to treat chronic diseases.[1] Furthermore the overall production costs for oral formulations are lower than those for parenteral formulations as there is no need for sterile manufacturing procedures,[1] making it more likely that an oral form of a drug is likely to reach a wider patient group. Nevertheless the development of successful and effective oral formulations is often challenging and issues such as instability in the gastrointestinal tract, poor dissolution in the gastrointestinal tract and poor permeability across the gastrointestinal epithelium often lead to unsatisfactory bioavailability data.[2] Also the oral bioavailability of a formulation not only depends on the amount of drug penetrating the gut mucosa, i.e., fraction absorbed, but also on the extent of drug metabolized during passage through the intestinal barrier (by the enzymes present in the gut wall) and the liver (where first pass metabolism occurs).[3,4]

The ability of a drug compound to dissolve in the gastrointestinal fluids is crucial, as permeation across the intestinal membrane must be preceded by dissolution for oral absorption to take place. For this reason, hydrophobic drugs have low oral bioavailability due to their poor solubility in the luminal fluids. In actual fact an unsuitable set of drug molecule physical properties leading to unsatisfactory drug pharmacokinetics is estimated to be responsible for up to 40% of drug development failures.[5]

The majority of drug candidates emerging from drug discovery programs are relatively hydrophobic as such hydrophobic compounds exhibit superior binding to receptor targets.[6,7] Although some degree of apolar character is considered important for drug absorption,[6] poor water solubility hinders absorption. In fact, nearly 50% of active substances being identified via high throughput receptor-based screening assays are either insoluble or poorly soluble in water, posing a significant challenge for drug development.[8] Measures taken to improve the solubility of hydrophobic drugs in order to optimize bioavailability include chemical modifications to form a more soluble salt[9] or prodrug,[10,11] reduction in particle size,[12,13] complexation with cyclodextrins,[14,15] the use of surfactants,[16] formulation of emulsions[17] and more

Received: April 13, 2011
Revised: October 25, 2011
Accepted: November 2, 2011
Published: November 2, 2011

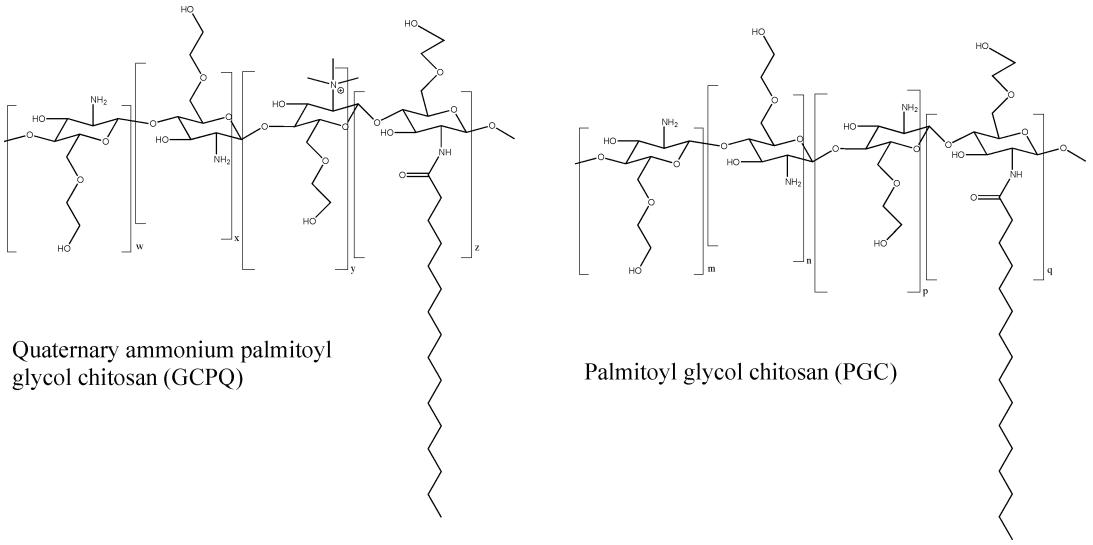

Figure 1. Quaternary ammonium palmitoyl glycol chitosan (GCPQ) and palmitoyl glycol chitosan (PGC).

recently the exploitation of the amphiphilic properties of polymers.[18,19]

The oral delivery of drugs with poor gastrointestinal permeability is also problematic, and strategies to improve the oral absorption of such hydrophilic low permeability compounds have included the formation of electrostatic complexes to effectively reduce the polarity of the molecules.[20]

Here we report on drug delivery nanoparticles (nanomedicines), which significantly enhance the oral absorption of hydrophobic and to lesser extent hydrophilic drugs and have elucidated the mechanism by which hydrophobic drug absorption is enhanced.

Amphiphilic polymers bearing pendant alkyl and acyl chains form highly stable self-assemblies in aqueous media, with critical micellar concentrations (CMCs) in the μM range,[21−23] as opposed to the CMC values in the mM range seen, for example, with the Pluronic block copolymers.[24] This makes the former amphiphiles prime candidates for use in drug delivery. Highly stable nanosystems will be less likely to prematurely disaggregate on dilution within biological fluids *in vivo* and, as a result will be able to transport their payload as intended. For example there is evidence that chitosan amphiphile [quaternary ammonium palmitoyl glycol chitosan (GCPQ)] nanoparticles increase the transport of hydrophobic drugs to the brain and across the cornea[21] and that poly(ethylenimine) amphiphile [quaternary ammonium cetyl poly(ethylenimine)] nanoparticles enhance the oral absorption of hydrophobic drugs.[18,19] We thus set out to study GCPQ nanoparticles as bioavailability enhancers and elucidated the mechanism of enhancement of hydrophobic drug absorption. We hypothesize that GCPQ nanoparticles, due to their ability to form highly stable self-assemblies,[21] would encapsulate hydrophobic drugs within the interior of the nanoparticle, promote dissolution due to the high surface area of the nanoparticle and promote transport through the gut epithelial cells via the transcellular route. We further hypothesize that gut epithelial transport will be promoted due to the fact that chitosan amphiphiles are bioadhesive[25] and the adherence of GCPQ nanomedicines to the mucous would enable the particles to enjoy a longer residence time within the absorptive upper gastrointestinal tract. Additionally the adherence of GCPQ nanomedicines to the gastrointestinal mucosa would result in intimate contact between the drug loaded nanoparticles and the absorptive enterocytes, thus minimizing the effect of the mucosal barrier. We set out to test the hypothesis using the model drugs cyclosporin A and griseofulvin, both Biopharmaceutical Classification (BCS) class II drugs with low water solubility and high gut permeability.[26] We also evaluated these chitosan amphiphile nanoparticles as permeability enhancers of hydrophilic drugs using ranitidine (a BCS class III drug with high water solubility and low gut permeability) as a model drug. Tissue imaging studies were undertaken with ex vivo samples taken from animals dosed with the fluorescent drug idarubicin; the BCS classification of idarubicin is not known.

EXPERIMENTAL SECTION

Materials. All reagents and chemicals were obtained from Sigma Aldrich Chemical Co., Poole, U.K., unless otherwise stated. All reagents and chemicals were used without further purification.

Synthesis of Chitosan Amphiphiles. Palmitoyl glycol chitosan (PGC)[27] and quaternary ammonium palmitoyl glycol chitosan (GCPQ)[21] (Figure 1) were synthesized as previously described. Briefly glycol chitosan (2 g) was degraded by dissolving in hydrochloric acid (4 M, 150 mL) and placed in a preheated water bath at 50 °C. After 24 h, the reaction was stopped and the product isolated and purified by exhaustive dialysis. Low molecular weight glycol chitosan (GC24) was recovered as a cream-colored cotton-wool-like solid: M_w = 10,159 Da, M_n = 8,386 Da, M_w/M_n = 1.283, dn/dc = 0.1405.

A further glycol chitosan sample (GC48) was prepared in a similar manner to that outlined above, except that the degradation time was extended to 48 h: M_w = 6,892 Da, M_n = 5,832 Da, M_w/M_n = 1.182, dn/dc = 0.1305.

Briefly PGC (PGC24 from GC24 and PGC48 from GC48) was synthesized from the degraded glycol chitosan by dissolving degraded glycol chitosan (500 mg) and sodium bicarbonate (Fluka, Poole, U.K., 376 mg) in a mixture of absolute ethanol (Fisher Scientific, Poole, U.K., 24 mL) and water (76 mL), to which was added dropwise a solution of palmitic acid *N*-hydroxysuccinimide (792 mg) dissolved in absolute ethanol (150 mL) with continuous stirring over a period of 1 h. The mixture was then stirred for 72 h and the product isolated by evaporating off most of the ethanol and

dx.doi.org/10.1021/mp200469a|*Mol. Pharmaceutics* 2012, 9, 14−28

extracting the remaining aqueous phase with diethyl ether (3 × 100 mL). The aqueous mixture of the polymer was exhaustively dialyzed (MWCO = 12−14 kDa) against water (5 L) with 6 changes over a period of 24 h. The resultant product (PGC) was freeze-dried to give a white cotton-like solid. PGC24: Yield = 445 mg, mole % palmitoylation = 49%. PGC48: Yield = 440 mg, % palmitoylation = 28%, ^{1}H NMR [$(CD_3)_2SO$, D_2O−9:1] δ = 0.85 [t, CH_3−$(CH_2)_{14}$−CO−], 1.25 [m, CH_3−$(CH_2)_{12}$−CH_2−CH_2−CO−], 1.50 [m, CH_3−$(CH_2)_{12}$−CH_2−CH_2−CO−], 2.00 [s, CH_3−CO−NH−], 2.20 [m, CH_3−$(CH_2)_{12}$−CH_2−CH_2−CO−], 2.5 = solvent, 2.6 (−CH(OH)−CH(NH_2)−), 2.7 (−CH−CH−NH−CO−), 3.2−4.2 (−CH−O), 4.4 solvent, 5.0 (O−CH−O anomeric proton).

GCPQ (GCPQ24 from PGC24 and GCPQ48 from PGC48) were synthesized by dispersing PGC (300 mg) in *N*-methyl-2-pyrrolidinone (Fisher Scientific, Poole, U.K., 25 mL) for 1 h at room temperature. Sodium hydroxide (40 mg), sodium iodide (45 mg) and methyl iodide (1 g) were added, and the reaction mixture was stirred under a stream of nitrogen at 36 °C for 3 h. Quaternary ammonium palmitoyl glycol chitosan (GCPQ) was recovered by precipitation with diethyl ether and the solid product washed with copious amounts of absolute ethanol. The resulting light brown solid was dissolved in water (100 mL) and the resulting yellow solution exhaustively dialyzed (MWCO = 12−14 kDa) against water (5 L) with 6 changes over a period of 24 h. The quaternary ammonium iodide salt was then passed through a column (Amberlite IRA-96 Cl^-, 1 × 6 cm) packed with one volume of the resin (30 mL) and subsequently washed with hydrochloric acid (1 M, 90 mL) followed by distilled water until a neutral pH was obtained. The clear eluate from the column was freeze-dried to give a transparent fibrous solid (GCPQ).

GCPQ24: Yield = 192 mg, M_w = 12,195 Da, M_n = 10,188, M_w/M_n = 1.197, d*n*/d*c* = 0.2380, mole % palmitoylation = 16 mol %, mole % quaternary ammonium groups = 8 mol %.

GCPQ48: Yield = 228 mg, M_w = 8,698 Da, M_n = 8,478, M_w/M_n = 1.030, d*n*/d*c* = 0.2515, mole % palmitoylation =16 mol %, mole % quaternary ammonium groups = 11 mol %.

^{1}H NMR (CD_3OD, D_2O−9:1] δ = 0.90 [t, CH_3-$(CH_2)_{14}$−CO−], 1.30 [m, CH_3−$(CH_2)_{12}$−CH_2−CH_2−CO−], 1.65 [m, CH_3−$(CH_2)_{12}$−CH_2−CH_2−CO−], 2.05 [s, CH_3−CO−NH−], 2.20−2.40 [b, CH_3−$(CH_2)_{12}$−CH_2−CH_2−CO−], 2.7−3.2 [b, −CH−CH−NH−CH_3− and −CH−CH−N$(CH_3)_2$], 3.30 = solvent, 3.45 [s −CH−CH−N$(CH_3)_3$], 3.50−4.40 (−CH−O), 4.50−5.00 (solvent, O−CH−O anomeric carbon).

^{1}H NMR analysis was carried out as previously described.[21,27] The level of palmitoylation was calculated by comparing the ratio of palmitoyl methyl protons (δ = 0.89−0.90) to sugar methine/methylene protons (δ = 3.5−4.5) and the level of quaternization calculated by comparing the ratio of quaternary ammonium methyl protons (δ = 3.45) to sugar methine/methylene protons.[21,28]

The molecular weight of PGC24 was estimated using the molecular weight of GC, determined as previously described,[27] and the level of palmitoylation (the latter determined using ^{1}H NMR data). The molecular weight of GCPQ was determined as detailed below. Specific refractive index increments (d*n*/d*c*) of GCPQ were measured in a mixture of acetate buffer [CH_3COONa (0.3 M), CH_3COOH (0.2 M), pH 5]:methanol (35:65) at 40 °C with an Optilab DSP interferometric refractometer (Wyatt Technology Corporation, USA) set at a wavelength of 690 nm. Filtered (0.2 μm) samples (0.1 to 1 mg mL^{-1}) were manually injected at a flow rate of 0.3 mL min^{-1} and the data obtained processed using DNDC for Windows version 5.90.03 software (Wyatt Technology Corporation, USA). The molecular weight of GCPQ was measured using gel permeation chromatography−multiangle laser light scattering (GPC−MALLS). Measurements were performed using a DAWN EOS MALLS detector (λ = 690 nm), Optilab DSP interferometric refractometer (λ = 690 nm) and a quasielastic light scattering (QELS) detector (Wyatt Technology Corporation, U.S.A.). Filtered samples of GCPQ (0.2 μm, 200 μL) were injected into a POLYSEP-GFC-P 4000 column (300 × 7.8 mm, Phenomenex, U.K.) fitted with a POLYSEP-GFC-P guard column (35 × 7.8 mm, Phenomenex, U.K.) using a Waters 717 Plus autosampler (Waters Corporation, Elstree, U.K.) at a loading concentration of 10 mg mL^{-1} with a flow rate of 0.8 mL min^{-1}. The data were analyzed using ASTRA for Windows version 4.90.08 software.

Self Assembly. Self-assembled polymer amphiphiles were prepared by probe sonication (Soniprep 150 Instruments, Sanyo, U.K) of PGC and GCPQ in aqueous media for 5 min with the instrument set at 75% of its maximum output. Self-assembly was probed using both the pyrene and methyl orange probes.[18,23,29]

A dilute aqueous solution of pyrene (2 μM) was prepared by first dissolving pyrene in ethanol (0.4 mg mL^{-1}). An aliquot of this pyrene solution (100 μL) was pipetted into a volumetric flask (100 mL), and the ethanol was evaporated off under a stream of nitrogen. The solution was then made up to 100 mL with distilled water. Using the aqueous pyrene solution as the solvent, polymer solutions of various concentrations (0.1 μg mL^{-1} to 10 mg mL^{-1}) were prepared by probe sonication and their fluorescence emission spectra recorded (exc. = 335 nm, Perkin-Elmer LS50-B, Perkin-Elmer Instruments, Cambridge, U.K.). The ratios of the intensity of the third (383 nm) and first (375 nm) vibronic peaks in the pyrene emission spectra (the I3/I1 ratio) were recorded,[29,30] and the critical micellar concentration was thus calculated.

A solution of methyl orange (25 μM) was prepared in borate buffer (0.02 M, pH 9.4) by dissolving methyl orange (1.64 mg) and borax (1.526 g) in distilled water (200 mL). Polymer dispersions were prepared (0.1 μg mL^{-1} to 10 mg mL^{-1}) in the methyl orange solution using probe sonication and polymer dispersions incubated at room temperature (25 °C) for 1 h before the absorption (350−600 nm) was recorded using the UV−vis spectrophotometer (Shimadzu, U.K.). The CMC of the polymers were recorded by monitoring the wavelength of maximum of absorbance of methyl orange.[18,23,29,31]

The heats of demicellization of the polymers[23] were measured using a VP-ITC MicroCalorimeter (MicroCal, LLC, Northampton, MA USA). The sample cell was filled with degassed ultrapure water. Concentrated polymer samples were loaded into a syringe (250 μL), and at 360 s intervals, polymer samples (10 μL) were injected into the sample cell and the heat flow was measured as a function of time. The syringe was rotated at 310 rpm to enable even mixing throughout the experiment. Data analysis was carried out using the MicroCal Origin version 7.0 Software. Each titration experiment was carried out at room temperature (25 °C).

Transmission electron microscopy with negative staining (1% w/v uranyl acetate aqueous solution)[22] was used to visualize polymer self-assemblies in the aqueous environment. A drop of sample was pipetted onto a support film followed by application of the negative stain. The images were captured using an energy

filtering electron microscope (FEI CM120 Bio Twin, Eindhoven, The Netherlands) operating at 120 kV.

Nanoparticle Drug Formulations. Various concentrations (4−40 mg mL^{-1}) of polymer dispersions in distilled water were prepared by probe sonication, as described above, and transferred to glass vials containing preweighed cyclosporin A or griseofulvin (10 mg). The hydrophobic drug was incorporated into the polymer aggregates by probe sonication (5 min with the instrument set at 75% of its maximum output). The cyclosporin A loaded formulations were stored at 2−8 °C overnight and analyzed the following day as cyclosporin A exhibits enhanced aqueous solubility at lower temperatures.[32] The drug encapsulated polymer formulations were filtered (0.45 μm) to remove unencapsulated drug particles and larger polymer−drug particles. The filtrate was dissolved in acetonitrile:water (1:1) and analyzed by HPLC as previously described.[18] Griseofulvin was analyzed using a Waters 515 HPLC pump, Waters 717 plus autosampler and Waters 486 tunable absorbance detector. Samples were chromatographed over a reverse phase column: Waters Asymmetry Spherisorb ODS2 (5 μm, 250 × 4.6 mm), maintained at a constant temperature with a Jones chromatography column heater model 7971(Fisher Scientific, Poole, U.K.) and eluted with an acetonitrile:water:acetic acid (700:300:1) mobile phase at a flow rate of 1.0 mL min^{-1} at 60 °C. The griseofulvin peak was detected at 292 nm with a retention time of 3.5 min. The data was analyzed using Waters Empower computer software. Calibration curves for cyclosporin A and griseofulvin (r^2 > 0.99) were obtained using various concentrations of standard solutions ranging from 0.5 to 10 μg mL^{-1}.

The long-term stability of the polymer drug nanoparticles was evaluated by storing GCPQ, cyclosporin A (20 mg mL^{-1}, 5 mg mL^{-1}) formulations, prepared as described above, except that probe sonication was carried out for 20 min. Prior to commencing the stability study, samples were stored at refrigeration temperatures (2−8 °C) for 24 h and subsequently filtered (0.45 μm). Samples either were stored as a freeze-dried cake at room temperature (16−25 °C) or were stored as liquid formulations at refrigeration temperatures. At regular intervals samples were filtered (0. 45 μm) to remove noncolloidal drug and analyzed (subsequent to reconstitution in the case of freeze-dried samples) by HPLC as described above.

Tablet formulations of the cyclosporin A nanoparticles were prepared by directly compressing the excipients and cyclosporin A (Table 1) using an EKO single punch tablet (5 mm) machine (Erweka, Heusenstamm, Germany). Tablets were prepared with a tablet hardness of 4−10 kg. Tablets were subjected to a disintegration test for uncoated tablets according to the specification laid down by the United States Pharmacopoeia (USP)[33] and a dissolution test using USP apparatus II (paddle method, Erweka DT6R Dissolution Tester) at a speed of 50 rpm and temperature of 37 °C.[33] Analysis of drug release was carried out by HPLC as described above.

Table 1. GCPQ−Cyclosporin A Tablet Formulations

tablet compositions	cyclosporin A tablets	GCPQ, cyclosporin A tablets
cyclosporin A	5	5
mannitol	100	100
avicel	100	100
stearic acid	5	5
sodium dodecyl sulfate	2	2
GCPQ	0	25

Oral Drug Absorption. *Cyclosporine.* The polymers (15 mg mL^{-1}) were formulated with cyclosporin A (2 mg mL^{-1}) in distilled water by probe sonication on ice (10 min with the instrument set at 75% of its maximum output). The formulations were stored overnight at 2−8 °C. The commercial formulation Neoral was diluted to a concentration of 2 mg mL^{-1} with distilled water. A suspension of cyclosporin A in water (2 mg mL^{-1}) was also prepared. Prior to oral administration, all formulations were analyzed by HPLC to determine the exact drug concentration for dose calculations. Male Wistar rats (weights = 200−250 g) were fasted for 12 h prior to dosing and for a further 4 h thereafter. The rats had free access to water throughout the study. Cyclosporin A (7.5 mg kg^{-1}) formulations (unfiltered) were given to rats by oral gavage in a single dose (~1 mL).[18] Blood samples were taken (~0.3 mL) at various time intervals, and a terminal blood sample was taken at 24 h by cardiac puncture. Cyclosporin A blood levels were analyzed using a specific monoclonal antibody radioimmunoassay kit (Cyclo-Trac SP-Whole Blood Radioimmunoassay Kit, Diasorin Inc., Bracknell, U.K.) in accordance with the manufacturer's instructions.

In some instances filtered (0.45 μm) cyclosporin A formulations were administered and cyclosporin A blood levels measured as detailed above. The amount of polymer in such filtered formulations was calculated using gravimetric analysis. The weights of empty vials and vials containing GCPQ (15 mg) were recorded. Polymer dispersions (15 mg mL^{-1}) were prepared in water, probe sonicated (10 min at 75% maximum output) and filtered (0.45 μm) as previously described. The filtrate was freeze-dried and weighed and the weight of GCPQ lost to filtration thus calculated. Similarly for cyclosporin A−GCPQ formulations, the amount of GCPQ and drug lost to filtration was measured using the gravimetric method to measure the total weight of solids lost to filtration and HPLC to determine the amount of drug lost to filtration. The amount of GCPQ lost to filtration of cyclosporin A−GCPQ formulations was thus calculated by difference.

Griseofulvin. The polymers (25 mg mL^{-1}) were formulated with griseofulvin (12.5 mg mL^{-1}) in distilled water by probe sonication (10 min with the instrument set at 75% of its maximum output) and orally administered as freshly prepared dispersions. Male Wistar rats (weights = 200−250 g) were given free access to food and water throughout the study. Griseofulvin (25 mg, 100−125 mg kg^{-1}) formulations with and without the polymer were administered to the rats by oral gavage in a single dose (~2 mL). Blood samples (~0.5 mL) were taken from the tail vein at various time intervals, and a terminal blood sample was taken at 24 h by cardiac puncture. Blood samples were centrifuged for 10 min at 2000 rpm (MSE Micro Centaur, MSE, London, U.K.), and the plasma was collected and frozen until analysis could be performed. Griseofulvin was extracted from the plasma samples by protein precipitation. Thawed plasma samples (0.3 mL) were diluted with acetonitrile (0.6 mL), the resulting mixture vortexed and probe sonicated for 2 min (with the instrument set at 75% of its maximum output) and centrifuged (10 min × 8000 rpm), and the supernatant collected into a glass vial and freeze-dried. The freeze-dried residue was reconstituted with mobile phase [acetonitrile:water:acetic acid (400:600:1) 200 μL] containing diazepam (0.2 μg mL^{-1}) as the internal standard. The samples

were analyzed using the Agilent Technologies 1200 series chromatographic system, which consisted of a vacuum degasser, a quaternary pump, a standard and preparative autosampler, a thermostated column compartment and a variable wavelength UV detector. The flow rate was set at 1.5 mL min^{-1}, samples (50 μL) were chromatographed over a reverse phase column (Sunfire C18 ODS2 5 μm, 4.6 × 250 mm) fitted with a guard column maintained at 60 °C, and samples were analyzed using a standard curve ($y = 36.79x - 0.0857$, $r^2 = 0.998$) with a concentration range of 0.1−1.0 μg mL^{-1}. The extraction efficiency for griseofulvin was 73.43 ± 8.81%. The griseofulvin and diazepam peaks were detected at 292 nm with retention times of 9.4 and 16.4 min respectively.

Ranitidine. The polymers (20 mg mL^{-1}) were formulated with ranitidine hydrochloride (10 mg mL^{-1}) in distilled water by probe sonication on ice for 5 min (with the instrument set at 75% of its maximum output). The formulations were stored overnight at 2−8 °C. The commercial formulation Zantac was diluted to a concentration of 10 mg mL^{-1} with distilled water. Prior to oral administration, all formulations were analyzed by HPLC to determine the exact concentration for dose calculations. Male Wistar rats (weights = 200−250 g) were allowed free access to food and water throughout the study. Ranitidine hydrochloride (50 mg kg^{-1}) formulations with and without the polymer were administered to the rats by oral gavage in a single dose (∼1 mL). Blood samples (∼0.5 mL) were taken from the tail vein at various time intervals, and a terminal blood sample taken at 24 h by cardiac puncture. Blood samples were centrifuged (10 min × 2000 rpm) and plasma was separated and frozen, until analysis could be performed. To thawed plasma samples (0.3 mL) was added sodium hydroxide (5 M, 0.3 mL), and the mixture was vortexed for 1 min. This was followed by the addition of ethyl acetate (0.5 mL), a further 2 min of vortexing and centrifugation for 10 min at 2000 rpm. The organic phase was transferred into a glass vial and freeze-dried and the freeze-dried residue reconstituted with the mobile phase [ammonium acetate (0.1 M):methanol: triethylamine, 700:300:1, 200 μL]. The samples were analyzed using the Agilent Technologies 1200 series chromatographic system as described above at a flow rate of 1 mL min^{-1}. Samples (50 μL) were chromatographed over a reverse phase column (Sunfire C18 ODS2 5 μm, 4.6 × 250 mm) fitted with a guard maintained at 40 °C. The extraction efficiency for ranitidine was 89.49 ± 9.49%, and samples were analyzed using a standard curve ($y = 110.6x - 12.98$, $r^2 = 0.999$) with a concentration range of 0.1−5.0 μg mL^{-1} and a UV detection wavelength of 320 nm. Ranitidine exhibited a retention time of 5.1 min.

Ex Vivo Confocal Laser Scanning Imaging. GCPQ was labeled with Texas Red (Invitrogen, Paisley, U.K.) using the protocol supplied by the manufacturer. Briefly GCPQ (100 mg) was dissolved in sodium bicarbonate buffer (0.1 M, 10 mL). Texas Red-X succinimidyl ester (5 mg) was dissolved in DMSO (0.5 mL) and was slowly added to the GCPQ solution with continuous stirring. The reaction mixture was incubated for 1 h at room temperature, and reaction was stopped by adding freshly prepared hydroxylamine (1.5M, 0.1 mL) to the mixture. The hydroxylamine containing reaction mixture was incubated for a further 1 h at room temperature, exhaustively dialyzed (5 L with 6 changes over a period of 24 h, MWCO = 12−14 kDa) and purified by column chromatography [Sephadex G-25 column (300 mm × 18 mm) eluted with water]. The reaction and purification mixtures were protected from light throughout the whole process. The attachment of the green fluorescent probe carboxyfluorescein to GCPQ was carried out using a similar protocol.

GPC−MALLS analyses was used to confirm the attachment of the fluorescent probes (Texas Red and carboxyfluorescein) to GCPQ as well as to ensure complete removal of unreacted dye from the labeled polymer. Filtered (0.2 μm) polymer samples (200 μL) were chromatographed over a POLYSEP-GFC-P 4000 column (300 × 7.8 mm, Phenomenex, Macclesfield, U.K.) fitted with a POLYSEP-GFC-P guard column (35 × 7.8 mm) using a Waters 717 Plus autosampler at a loading concentration of 5−10 mg mL^{-1} with a flow rate of 1 mL min^{-1}. Detection was carried out via a Wyatt system: DAWN EOS MALLS detector (λ = 690 nm), Optilab DSP interferometric refractometer (λ = 690 nm) and a QELS detector. The mobile phase was a mixed solvent of acetate buffer [CH_3COONa (0.3M), CH_3COOH (0.2 M), pH 5]:methanol (35:65). Data were analyzed using ASTRA for Windows version 4.90.08 software. There were no residual unreacted fluorescent dye peaks in the GCPQ−Texas Red or GCPQ−carboxyfluorescein chromatograms (Figure 1 in the Supporting Information).

Texas Red−GCPQ (15 mg mL^{-1}, ∼1 mL, 75 mg kg^{-1}) in distilled water was dosed to male Wistar rats (weight = 200−250 g) by oral gavage. A separate group of rats were orally dosed with idarubicin (2 mg mL^{-1}, ∼1 mL, 10 mg kg^{-1}) with and without GCPQ/GCPQ−carboxyfluorescein (15 mg mL^{-1}, ∼1 mL, 75 mg kg^{-1}). At various time points animals were killed and their intestines harvested. The small intestine was divided into three sections, the duodenum (up to ∼8 cm from the stomach), jejunum (the next ∼30 cm) and ileum (the next ∼20 cm).[34] Each section was cut along its long axis, opened flat, rolled along its long axis, embedded in optimal cutting temperature (OCT) compound and frozen in liquid nitrogen. This procedure was carried out as quickly as possible (i.e., within 10 min) to avoid the tissue deterioration. The tissues were sectioned into thin slices (10 μm) using a cryostat (Leica CM1850) set at −25 °C. The slices were placed on poly-L-lysine microscope adhesion slides and fixed with freshly prepared paraformaldehyde (0.4% w/v) in phosphate buffered saline (pH = 7.4, PBS). The slides were soaked in PBS for 10 min, followed by antifade agent, Citifluor AF1. A coverslip was placed on the slide, and the edges were sealed with nail polish. Slides were imaged using a Zeiss LSM 510 laser scanning confocal microscopy imaging system, equipped with an argon ion laser (LASOS Laserteknik GmbH, Carl Zeiss Promenade 10) and linked to a Fujitsu Siemens computer with the LSM 510 version 3.2 software (red fluorescence excitation wavelength = 543 nm, green fluorescence excitation wavelength = 488 nm).

In Vitro Mechanistic Studies. In order to examine the effect of the polymer nanoparticles on the integrity of the intercellular tight junctions, the transepithelial electrical resistance (TEER) and transport properties of a Caco-2 cell monolayer were monitored in the presence of GCPQ nanoparticles. Caco-2 cells (passage number 50−60) were seeded on 12-well plates with polycarbonate permeable cell culture inserts (area 1 cm^2, pore diameter 0.4 μm) at a seeding density of 64000 cells cm^{-2}. Dubelcco's modified Eagle's medium (DMEM, Invitrogen, Paisley, U.K.) supplemented with fetal bovine serum (FBS 10% w/v), nonessential amino acids (1% w/v), L-glutamine (1% w/v), penicillin (100U mL^{-1}) and streptomycin (100 μg mL^{-1}) were used as the culture medium and added to the basolateral

Table 2. Critical Micellar Concentration and Thermodynamics of Micellization of PGC and GCPQ

polymer	pyrene emission meth (mM)	methyl orange abs meth (mM)	ITC meth (mM)	ΔG_{mic} (kJ mol^{-1})	ΔH_{mic} (kJ mol^{-1})	$T\Delta S_{mic}$ (kJ mol^{-1})
PGC24	0.008	0.036	0.003	−41.4	−0.36	+41.1
GCPQ24	0.046	0.021	0.019	−36.9	+0.96	+37.9
GCPQ48	0.087	0.026	0.020	−36.9	+0.36	+37.3

compartments. Cell suspension in the same medium (0.5 mL) was added to the apical compartments, and the cells were incubated at 37 °C in an atmosphere of 95% relative humidity and 10% CO_2. The cells were maintained for 21 days to allow a confluent monolayer to develop. The culture media in both the apical and basolateral compartments were changed every other day. TEER measurements were performed and transport studies were conducted 21 days postseeding, after confirming the integrity of the monolayers.

The TEER of the Caco-2 cell monolayers was measured using a Millicell-ERS meter (Millipore, Bedford, MA, USA). Polymer dispersions (5 mg mL^{-1}) were prepared in Hanks balanced salt solution (HBSS) containing Ca^{2+} and Mg^{2+} supplemented with penicillin (100U mL^{-1}) and streptomycin (100 μg mL^{-1}). The culture medium was first aspirated from the Transwells, HBSS was added into both the apical and basolateral compartments, and the cells were incubated for an hour at 37 °C in an atmosphere of 95% humidity and 10% CO_2. The TEER of the cells in HBSS was then measured prior to the addition of the polymer dispersions (0.5 mL) in the apical compartments. TEER measurements were carried out at 40 min intervals. After 160 min, the polymer dispersions were removed and replaced with fresh HBSS and the TEER was measured again after removal of the polymer dispersions. HBSS and PEI (25 kDa) solutions were used as negative and positive controls respectively.

The transport kinetics of a paracellular transport marker (Lucifer Yellow) were also measured in the presence and absence of GCPQ nanoparticles. Polymer dispersions (5 mg mL^{-1}) were prepared in HBSS containing Lucifer Yellow (0.5 mg mL^{-1}). The culture medium was aspirated off and replaced with HBSS containing Ca^{2+} and Mg^{2+} supplemented with penicillin (100 U mL^{-1}) and streptomycin (100 μg mL^{-1}) in the basolateral compartments. Polymer dispersions with Lucifer Yellow were added to the apical compartments, and the Transwells were incubated at 37 °C, 95% humidity and 10% CO_2 for 160 min. Basolateral samples (1 mL) were taken every 40 min and replaced with equal volumes of fresh HBSS, and fluorescence readings (excitation wavelength = 485 nm, emission wavelength = 530 nm) were recorded. Lucifer Yellow concentrations were determined with reference to a calibration curve using standard solutions (0.2−20 μg mL^{-1}) for the fluorescence emission (y = 4.917x + 8.7023, r^2 > 0.99), and control samples (generated in the absence of polymer nanoparticles) were also analyzed.

The effect of GCPQ nanoparticles on transcellular transport was also analyzed. GCPQ dispersions (5 mg mL^{-1}) were prepared in HBSS containing antipyrine (0.4 mg mL^{-1}). The culture medium was aspirated off and replaced with HBSS containing Ca^{2+} and Mg^{2+} supplemented with penicillin (100 U mL^{-1}) and streptomycin (100 μg mL^{-1}) in the basolateral compartments. GCPQ−antipyrine dispersions were added to the apical compartments, and the Transwells were incubated at 37 °C, 95% humidity and 10% CO_2 for 160 min. Basolateral samples (0.5 mL) were taken every 40 min and replaced with equal volumes of fresh HBSS, and the concentration of antipyrine was analyzed by HPLC. Samples (20 μL) were chromatographed over two Onyx Monolithic C18 5 μm columns (2 × 100 × 4.6 mm) using Agilent Technologies HPLC 1200 series equipment. Columns were fitted with a guard column maintained at 30 °C in the thermostated column compartment (Agilent Technologies 1200 series) at a flow rate of 1.5 mL min^{-1}. Samples were eluted with a methanol, water (30:70) mobile phase, and antipyrine was detected at a wavelength of 254 nm and had a retention time of 5.0 min. The data was analyzed using the Agilent Chemstation Software and a calibration curve (y = 27.738x − 1.0777, r^2 = 0.9997) prepared with standard solutions (0.5−10 μg mL^{-1}).

To investigate the influence of GCPQ nanoparticles on the gastrointestinal efflux transporters (e.g., the P-glycoprotein efflux pump), the transport of rhodamine-123 across Caco-2 monolayers in the presence and absence of GCPQ nanoparticles was also evaluated. Verapamil[35] was included as a positive control. Polymer dispersions (1 mg mL^{-1}) were prepared in HBSS containing rhodamine-123 (5 μM). Verapamil (100 μM, 49 μg mL^{-1}) was also prepared with rhodamine-123 and used as a positive control. The culture medium was aspirated off and replaced with HBSS containing Ca^{2+} and Mg^{2+} supplemented with penicillin (100 U mL^{-1}) and streptomycin (100 μg mL^{-1}) in the basolateral compartments. GCPQ−rhodamine-123, rhodamine-123 alone, or rhodamine-123 + verapamil were added to the apical compartments and the Transwells incubated at 37 °C, 95% humidity and 10% CO_2 for 90 min. Basolateral samples (1 mL) were taken after 90 min incubation, the fluorescence was measured (excitation wavelength = 485 nm, excitation wavelength = 530 nm) and rhodamine-123 concentration was determined using standard solutions (0.05−1.0 μg mL^{-1}) and the fluorescence emission standard curve (y = 653.64x + 27.177, r^2 > 0.99). In a separate experiment, rhodamine-123 formulations were placed in the basolateral compartment with the polymer solutions and verapamil added to the apical side. Apical samples were taken after 90 min of incubation at 37 °C, 95% humidity and 10% CO_2, and the fluorescence was measured as previously described.

Statistical Analyses. Statistical significance was tested with one-way analysis of variance ANOVA using MINITAB 15 Statistical Software. In some cases, the statistical difference between two populations were compared using the Student's t test (Microcal Origin 6.0.)

RESULTS

Amphiphile Synthesis and Self Assembly. The synthesis and characterization of PGC[27,36] and GCPQ[21,28] have been reported previously, and both polymers are known to self-assemble in aqueous media, with PGC producing bilayer vesicles in the presence of cholesterol.[27,36] However while the critical micellar concentration (CMC) for various GCPQ variants has been recorded,[21] this is the first record of the CMC of PGC. GCPQ CMC values are dictated by the level of hydrophobic substitution on the polymer with the more hydrophobic molecules exhibiting lower CMC values.[21] Lower molecular weight GCPQ variants also have higher CMC values.[21] GCPQ CMC values range from 6 to 100 μM.[21]

dx.doi.org/10.1021/mp200469a|Mol. Pharmaceutics 2012, 9, 14−28

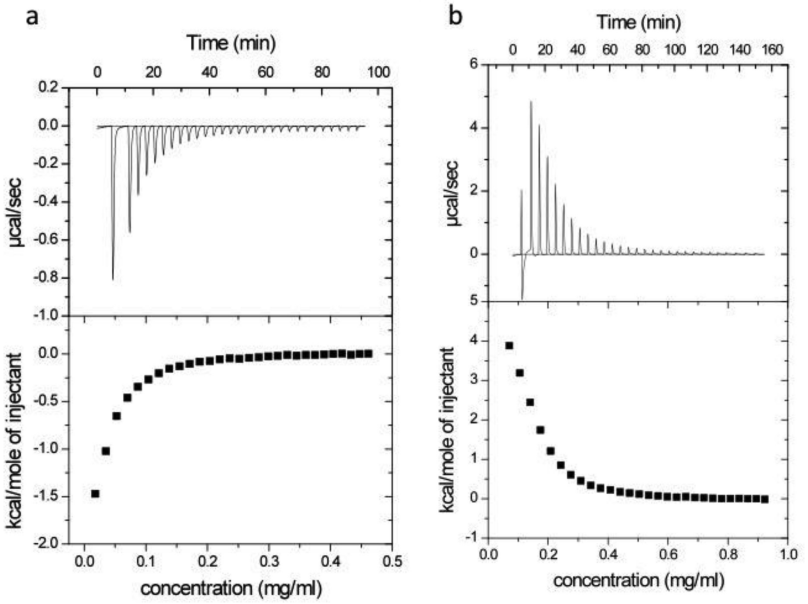

Figure 2. Dilution (demicellization) enthalpograms for an aqueous dispersion of (a) PGC24, (b) = GCPQ24.

Three methods were used to determine the CMCs of GCPQ and PGC: monitoring the pyrene emission spectra (Figure 2a in the Supporting Information), monitoring the UV absorption spectra (Figure 2b in the Supporting Information) and measuring the enthalpy change of demicellization (Table 2, Figure 2). The first two methods involved the use of hydrophobic probes (pyrene and methyl orange),[30,31] and the third—ITC—is a probe free method. All polymers aggregate in the low micromolar range and thus produce extremely stable self-assemblies, when compared to the majority of amphiphilic polymers, e.g. compared to the Pluronic amphiphiles of similar molecular weight (Pluronic F127 CMC = 0.55 mM).[37] The very low CMC values will enable the nanoparticles to resist disaggregation on dilution within the gastrointestinal tract following oral administration. There was good agreement between the ITC and pyrene CMC data, however the methyl orange PGC CMC data was higher than that recorded using other techniques. We have previously reported that the ITC probe free method is the most reliable method of measuring the CMC.[23]

Polymer aggregation is driven by the entropy gain (Table 1) experienced by liberated water molecules on association of the hydrophobic pendant groups of the polymer.[38] The entropy gain on micellization experienced by the chitosan amphiphiles [$T\Delta S$ = +37 to +41 kJ mol^{-1} (Table 2)] exceeds that experienced by Pluronic F127 ($T\Delta S$ = +25 kJ mole^{-1}),[37] a polymer of similar molecular weight (12.5 kDa), and this exceptionally high $T\Delta S$ value is responsible for their exceptional stability. PGC exhibited a greater tendency toward aggregation when compared to GCPQ, due to the higher level of hydrophobic substitution on this polymer.

PGC24 formed a cloudy dense dispersion while GCPQ formed a clear liquid. PGC[27] and GCPQ (Figure 3) dispersions presented as spherical polydisperse aggregates ranging from 40−200 nm in size. We speculate that particle formation is presumed to commence with polymer molecules aggregating into micellar self-assemblies of 40 nm size, followed by further aggregation of micellar particles with these multimicellar aggregates reorganizing to form the larger 100−200 nm particles. There were no morphological differences between GCPQ24 and GCPQ48 nanoparticles (data not shown).

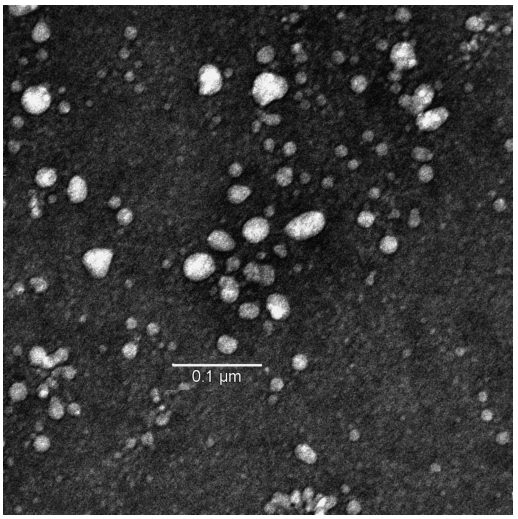

Figure 3. Transmission electron micrograph of GCPQ24 (10 mg mL^{-1}) nanoparticles in water.

Drug Formulation. On drug incorporation larger aggregates were formed (Figure 4). When comparing GCPQ to PGC drug nanoparticles, GCPQ24 and GCPQ48 encapsulated more drug within the colloidal fraction than the more hydrophobic polymer PGC24 (Figure 4a,b). It appears that the larger PGC24 polymer−drug self-assemblies (Figure 4g,h) were filtered out during the filtration step described above with particles of less than 400 nm in size encapsulating very little drug. At higher PGC24 concentrations (>20 mg mL^{-1}), progressively larger aggregates formed which could not be filtered out, limiting data collection at these polymer concentrations.

GCPQ formulations reveal 20−50 nm micelles and 100−500 nm particles in the unfiltered and filtered drug formulations (Figure 4c−f), with crystals of unencapsulated drug being observed in the unfiltered griseofulvin formulation (Figure 4f). Cyclosporine nanoparticles are remarkably stable, with drug

remaining entrapped for up to 6 months within the nanoparticles (Figure 4i) when the product was freeze-dried or stored as the liquid formulation. On incorporation of GCPQ into cyclosporin A tablets, the dissolution rate of cyclosporin A is enhanced by 60% (Figure 4j), despite GCPQ causing disintegration times to double. It is possible that the inclusion of superior disintegrating agents could promote dissolution rates further. GCPQ24, by forming polymeric micelles of cyclosporin A, facilitates the dissolution of cyclosporin A from the tablet dosage forms. The dissolution phenomenon recorded in Figure 4j involves release of GCPQ−cyclosporin A micelles from the tablet dosage form and eventually release of molecular drug from the micelles. It is widely acknowledged that only the dissolved drug will be absorbed and so dissolution of the dosage form within the finite gut residence time is desirable.

In Vivo Oral Absorption Studies. The oral absorption of cyclosporin A, a Biopharmaceutical Classification System class II drug with high gut permeation but low aqueous solubility[39] was significantly enhanced by administration as unfiltered GCPQ24 nanoparticles, when compared to either the drug alone in water or the commercial Neoral formulation (Figure 5a). In the case of unfiltered PGC24 and GCPQ48 formulations, the oral absorption profile was similar to that seen with the commercial formulation Neoral, but oral absorption was

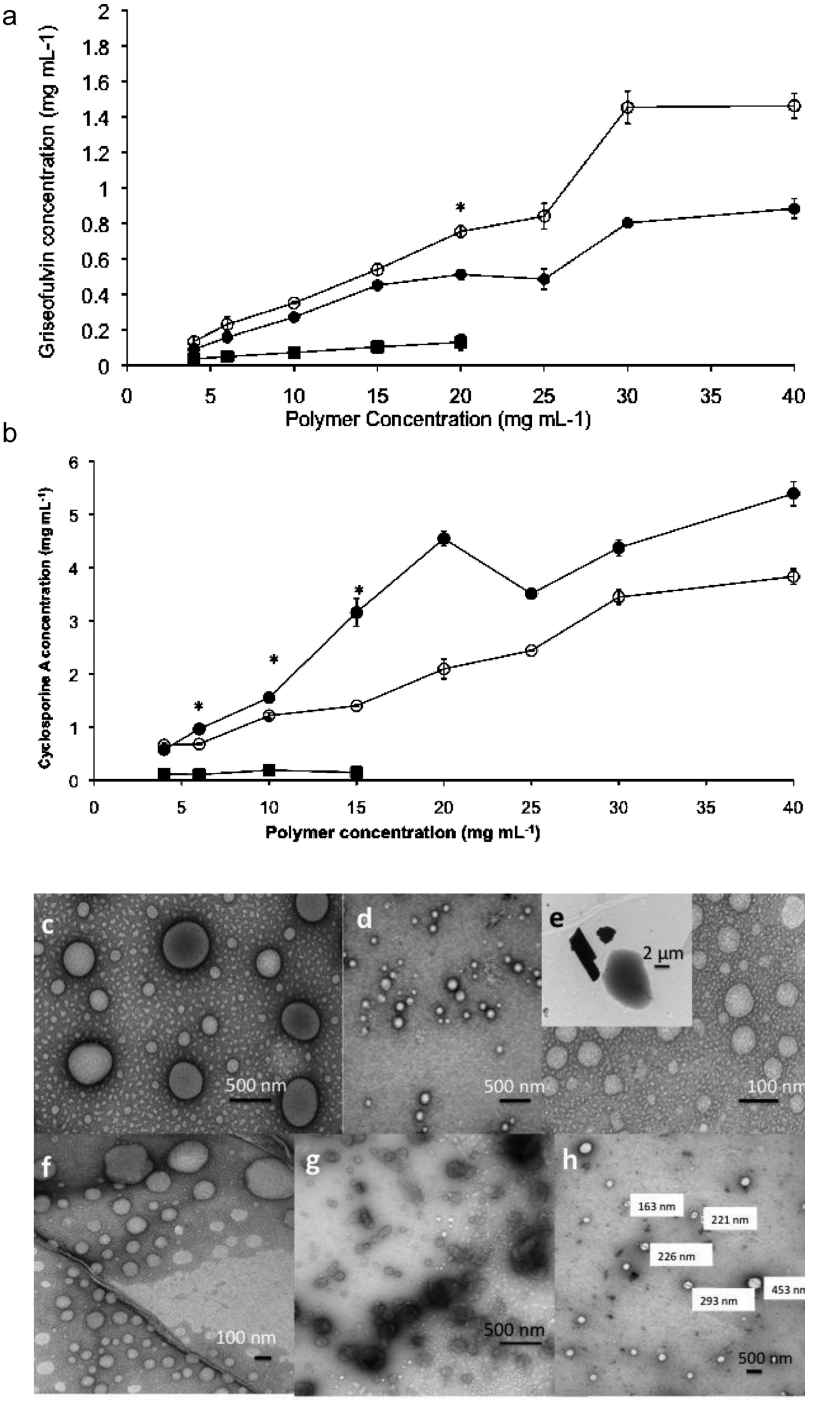

Figure 4. continued

dx.doi.org/10.1021/mp200469a | *Mol. Pharmaceutics* 2012, 9, 14–28

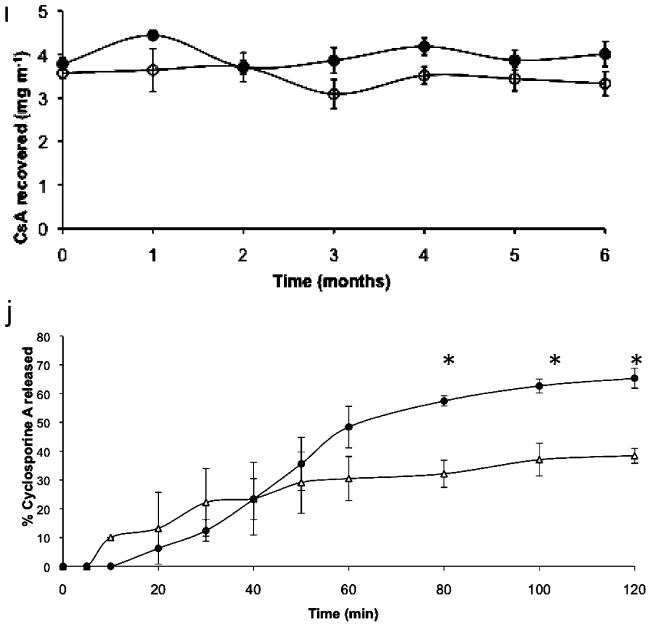

Figure 4. (a) Griseofulvin encapsulation into self-assembled polymer nanoparticles: ○ = GCPQ48, ● = GCPQ24, ■ = PGC24, initial griseofulvin concentration = 10 mg mL^{-1}; formulations were prepared by probe sonication followed by filtration (0.45 μm); the polymer concentration term refers to the initial concentration; * = significant differences between all polymers ($p < 0.05$). (b) Cyclosporin A encapsulation into self-assembled polymer nanoparticles: ● = GCPQ24, ○ = GCPQ48, ■ = PGC24 initial cyclosporin A concentration =10 mg mL^{-1}; formulations were prepared by probe sonication followed by filtration (0.45 μm); the polymer concentration term refers to the initial concentration; * = significant differences between all polymers ($p < 0.05$). (c–g) Transmission electron micrographs of drug formulations: (c) freshly prepared unfiltered GCPQ24–cyclosporin A (15 mg mL^{-1}:2 mg mL^{-1}) nanoparticles in water, (d) freshly prepared filtered (0.45 μm) GCPQ24–cyclosporin A (5 mg mL^{-1}: 2 mg mL^{-1}) nanoparticles in water, (e) freshly prepared unfiltered GCPQ24–griseofulvin (25 mg mL^{-1}:12.5 mg mL^{-1}) nanoparticles in water (inset shows crystalline material present in the formulation), (f) freshly prepared filtered (0.45 μm) GCPQ24–griseofulvin (25 mg mL^{-1}:0.4 mg mL^{-1}) nanoparticles in water, (g) freshly prepared unfiltered PGC24–cyclosporin A (5 mg mL^{-1}:1 mg mL^{-1}) nanoparticles in water, (h) freshly prepared filtered (0.45 μm) PGC24–cyclosporin A (5 mg mL^{-1}:0.1 mg mL^{-1}) nanoparticles in water. (i) The stability of GCPQ24–cyclosporin A nanoparticles. Formulations were prepared as described in the text, and samples were stored as either liquid formulations (●) at refrigeration temperature or as the freeze-dried cake (○) at room temperature for 6 months. There was no significant loss of drug within the nanoparticles after six months (nanoparticles were isolated prior to analyses by filtration through a 0.45 μm filter ensuring that only the drug content of the colloidal fraction was measured). (j) The effect of GCPQ24 on the dissolution of cyclosporin A from a tablet dosage form: ● = tablet formulation containing cyclosporin A (5 mg) and GCPQ24 (25 mg), Δ = tablet formulation containing cyclosporin A (5 mg); all other tableting excipients are contained in Table 1; * = statistical significance ($p < 0.05$). Tablet disintegration times = 8.3 ± 0.6 and 4 ± 1 min in the presence and absence of GCPQ24 respectively.

enhanced with both PGC24 and GCPQ48 nanoparticles when compared to the administration of cyclosporin A alone. The C_{max} was increased almost 5-fold (increased by 380%) when GCPQ24 was compared to the drug in water. The C_{max} was increased almost 2-fold (increased by 80%) when compared to the commercial formulation Neoral (Table 4). The C_{max} of GCPQ48 formulations was not significantly superior to the C_{max} obtained with Neoral (Figure 5a), indicating that the higher molecular weight GCPQ24 was a more efficient delivery system. The superior delivery characteristics of GCPQ24 could be due to the fact that GCPQ24 encapsulates more cyclosporin A within the colloidal fraction when compared to GCPQ48 (Figure 4b), demonstrating that encapsulation within the polymer particles is central to the bioavailability enhancement observed. The T_{max} was unchanged at 4 h (Table 4) irrespective of the formulation and was consistent with earlier reports.[40] Although some of the GCPQ24–cyclosporin A particles were 700 nm in size (Figure 4c), these polymer particles still had absorption enhancing properties when compared to the administration of the drug in water (Figure 5a).

The polymer was essential for the oral bioavailability enhancement as when filtered formulations, containing a lower level of polymer (Table 3) and smaller particles (Figure 4d), were administered there was no enhancement in the oral bioavailability of cyclosporin A, when compared to the drug in water (Figure 5b, Table 4). Filtration appears to remove GCPQ24 from the formulation, presumably by adherence of the polymer to the filter membrane and in essence an extraction of the polymer from the formulation is observed.

The oral absorption of griseofulvin, a BCS class II drug,[26] was significantly enhanced when the drug was administered as GCPQ24 and PGC24 nanoparticles (Figure 5c). The plasma C_{max} of griseofulvin was increased almost 6-fold (increased by 480%) by GCPQ nanoparticles and increased 2-fold (increased by 102%) by PGC24 (Figure 5c, Table 4). There was no significant difference in the oral absorption activity of both GCPQ nanoparticles. Despite the fact that the GCPQ24 griseofulvin formulation contained some unencapsulated crystalline material (Figure 4e), this polymer still significantly increased the bioavailabilty of griseofulvin when compared to the drug in solution (Figure 5c). Oral absorption from filtered GCPQ–griseofulvin formulations was not studied.

Ranitidine hydrochloride is a BCS class III drug[41] with high water solubility, low gastrointestinal membrane permeability and a bioavailability of 56% in humans.[42] Ranitidine hydrochloride is a suitable model compound for evaluating the ability of these nanoparticles to improve the gut permeability to hydrophilic compounds. As can be seen from Figure 5d and

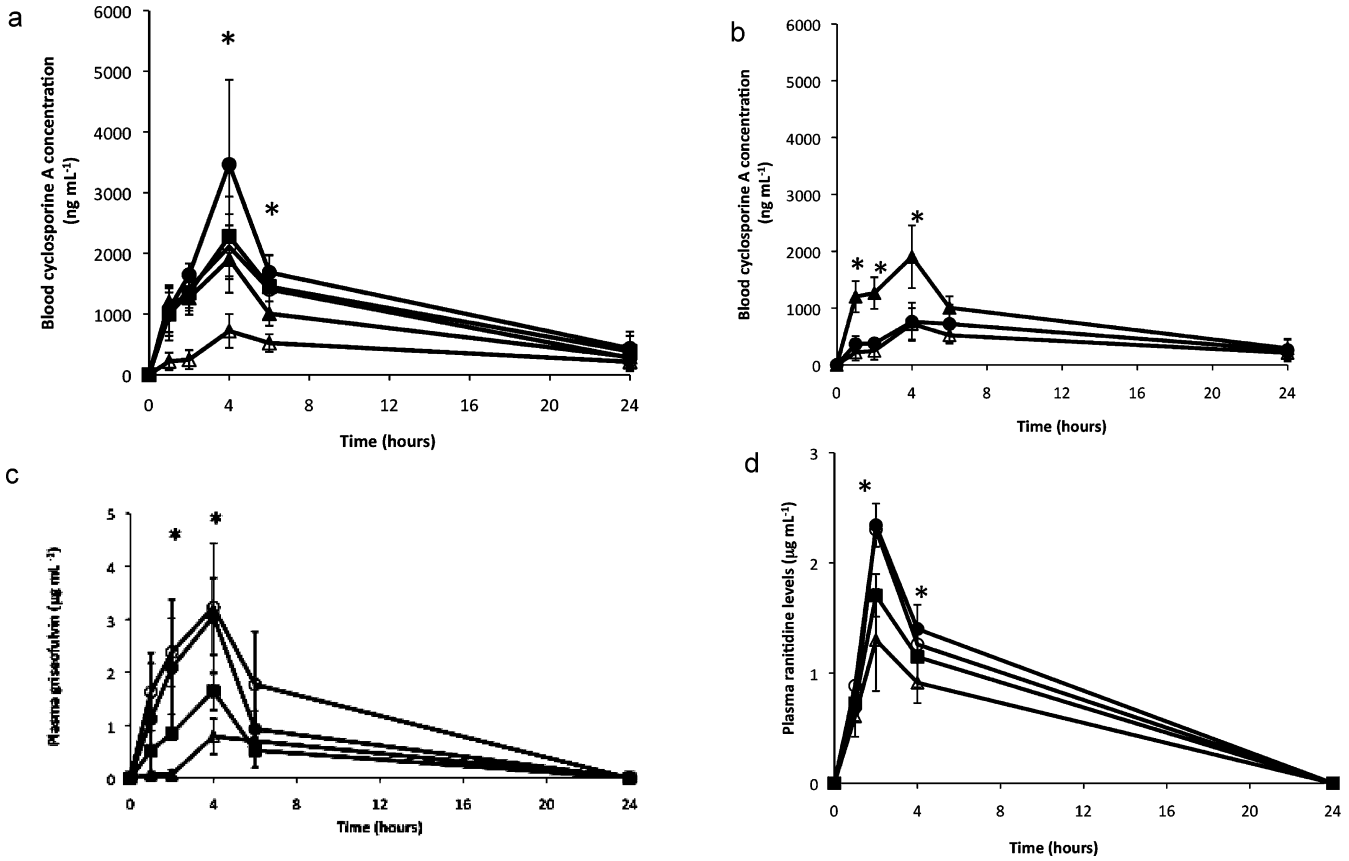

Figure 5. (a) Blood concentrations of cyclosporin A after the oral administration of cyclosporin A (7.5 mg kg^{-1}) formulations: polymer dose = 56.3 mg kg^{-1}, ● = cyclosporin A, GCPQ24 (2 mg mL^{-1}, 15 mg mL^{-1}), ○ = cyclosporin A, GCPQ48 (2 mg mL^{-1}, 15 mg mL^{-1}), ■ = cyclosporin A, PGC24 (2 mg mL^{-1}, 15 mg mL^{-1}), ▲ = Neoral (cyclosporin A = 2 mg mL^{-1}), Δ = cyclosporin A in water (2 mg mL^{-1}), * = significant differences between GCPQ24 and Neoral ($p < 0.05$); all formulations are significantly superior to cyclosporin A in water. (b) Blood concentrations of cyclosporin A after the oral administration of cyclosporin A (7.5 mg kg^{-1}) formulations: ● = filtered (0.45 μm) cyclosporin A–GCPQ24 (2 mg mL^{-1}, 5 mg mL^{-1}) formulation, GCPQ24 dose = 19 mg kg^{-1}, ▲ = Neoral (cyclosporin A = 2 mg mL^{-1}), Δ = cyclosporin A in water (2 mg mL^{-1}), * = significant differences between Neoral and all other formulations ($p < 0.05$). Filtration removes the bulk of the large particles and a large proportion of the GCPQ24 (Table 3). (c) Plasma concentrations of griseofulvin after the oral administration of griseofulvin (110 mg kg^{-1}) formulations: polymer dose = 220 mg kg^{-1}, ● = griseofulvin, GCPQ24 (25 mg mL^{-1}, 50 mg mL^{-1}), ○ = griseofulvin, GCPQ48 (25 mg mL^{-1}, 50 mg mL^{-1}), ■ = griseofulvin, PGC24 (25 mg mL^{-1}, 50 mg mL^{-1}), Δ = griseofulvin in water (25 mg mL^{-1}), * = significant differences between GCPQ and all other formulations ($p < 0.05$). (d) Plasma concentrations of ranitidine hydrochloride after the oral administration of ranitidine (50 mg kg^{-1}) formulations: polymer dose = 100 mg kg^{-1}, ● = ranitidine, GCPQ24 (10 mg mL^{-1}, 20 mg mL^{-1}), ■ = ranitidine, PGC24 (10 mg mL^{-1}, 20 mg mL^{-1}), ○ = ranitidine, GCPQ48 (10 mg mL^{-1}, 20 mg mL^{-1}), Δ = ranitidine in water (10 mg mL^{-1}), * = significant differences between GCPQ and ranitidine in water ($p < 0.05$).

Table 3. The Effect of Filtration (0.45 μm) on GCPQ24 Formulations

		cyclosporin A–GCPQ24 formulations				
GCPQ24 alone		GCPQ		cyclosporin A		
before[a]	after[b]	before	after	before	after	ratio after[c]
15	10.79	15	5.05	2	2.07	5:2

[a]Amount before filtration. [b]Amount after filtration. [c]Final GCPQ: cyclosporin A ratio after filtration.

Table 4, the GCPQ formulations increased the C_{max} by 80%. The PGC formulation was not significantly different from ranitidine hydrochloride alone. While the ability of GCPQ to significantly promote the oral absorption of the hydrophilic BCS class III compound ranitidine hydrochloride and thus improve gut permeability was proven, it must be acknowledged that there was no significant difference in the oral absorption profiles of the GCPQ formulations and the diluted Zantac syrup (Table 4). The diluted Zantac syrup contained 4.5%w/v ethanol.[43]

In order to investigate the mechanism of action of GCPQ in promoting oral absorption, rats were dosed with GCPQ–Texas Red and the gastrointestinal membrane imaged using confocal laser scanning microscopy (Figure 6). Two assumptions were made during this experiment, first that the attachment of a fluorescent label did not alter the behavior of GCPQ in the gastrointestinal tract, and second that the dye was not cleaved by any intestinal enzymes. Figure 5 shows that the red fluorescent signal from Texas Red was seen lining the villi, adhering to the mucosal surface of the villi, and was not detected within the cells of the villi. The ileum from a control rat dosed with water was also imaged (Figure 3 in the Supporting Information), and the red fluorescent signal was not detected. In order to prove that the fluorescent signal from any absorbed polymer would be visible within the cells of the villi, animals were dosed with the red fluorescent drug idarubicin and with GCPQ–carboxyfluorescein which produced a green

dx.doi.org/10.1021/mp200469a|*Mol. Pharmaceutics* 2012, 9, 14–28

Table 4. Pharmacokinetic Parameters after the Oral Administration of Cyclosporin A, Griseofulvin and Ranitidine Formulations

formulations	T_{max} (h)	C_{max} (μg mL^{-1})
Cyclosporin A (7.5 mg kg^{-1})		
Neoral	4	1.904 ± 0.554
cyclosporin A suspension	4	0.721 ± 0.227
unfiltered GCPQ24–cyclosporin A (7.5:1 g g^{-1}) nanoparticle formulations	4	3.465 ± 1.395
unfiltered PGC24–cyclosporin A (7.5:1 g g^{-1}) nanoparticle formulations	4	2.278 ± 0.656
filtered GCPQ24–cyclosporin A (2.5:1 g g^{-1}) nanoparticles	4	0.759 ± 0.334
unfiltered GCPQ48–cyclosporin A (7.5:1 g g^{-1}) nanoparticle formulations	4	2.110 ± 0.534
Griseofulvin (110 mg kg^{-1})		
griseofulvin suspension	4	0.528 ± 0.217
unfiltered GCPQ24–griseofulvin (2:1 g g^{-1}) nanoparticle formulations	4	3.051 ± 0.724
unfiltered PGC24–griseofulvin (2:1 g g^{-1}) nanoparticle formulations	4	1.066 ± 0.165
unfiltered GCPQ48–griseofulvin (2:1 g g^{-1}) nanoparticle formulations	4	3.223 ± 1.213
Ranitidine (50 mg kg^{-1})		
ranitidine	2	1.299 ± 0.453
unfiltered GCPQ24–ranitidine (2:1 g g^{-1}) formulations	2	2.342 ± 0.197
unfiltered PGC24–ranitidine (2:1 g g^{-1}) formulations	2	1.705 ± 0.193
unfiltered GCPQ24–ranitidine (2:1 g g^{-1}) formulations	2	2.303 ± 0.418
Zantac syrup	2	2.393 ± 0.858

fluorescent signal. As can be seen from Figure 6k–m, the red fluorescence emanating from idarubicin is present within the cells of the villi while the green fluorescent signal emanating from GCPQ is once again seen adhering to the mucus and lining the villi (Figure 6m). Furthermore GCPQ increases the amount of idarubicin seen inside the villi (Figure 6k,l), evidence that GCPQ promoted the absorption of idarubicin. These data (Figure 6) indicate that GCPQ is not appreciably orally absorbed despite the fact that the polymer enhances the oral absorption of both hydrophobic and hydrophilic drugs (Figure 5 and Table 4). Presumably this polymer mucoadhesion ensures a close proximity between the absorptive enterocytes and the polymer–drug, essentially traversing the mucosal barrier. Once again the gastrointestinal epithelia of rats dosed with water only did not reveal a fluorescent signal (Figure 6n; Figures 4a,c–g in the Supporting Information). Finally the polymer was examined for its propensity to lyse cells as some amphiphilic absorption enhancers, which promote dissolution within the gastrointestinal tract, also cause membrane damage. As demonstrated in Figure 7a, while polysorbate 80 is indeed hemolytic, GCPQ24 is nonhemolytic up to a concentration of 5 mg mL^{-1}.

In Vitro Mechanistic Studies. Having established that GCPQ significantly enhances the oral absorption of hydrophobic drugs (Figure 5a,c), increases the dissolution of a hydrophobic drug from a tablet dosage form (Figure 4j), and also enhances the absorption of hydrophilic drugs (Figure 5d), we then decided to investigate the mechanism of action of this polymer.

In the first instance we examined the influence of the polymer on the integrity of tight intercellular junctions using the Caco-2 cell monolayer model and an evaluation of the

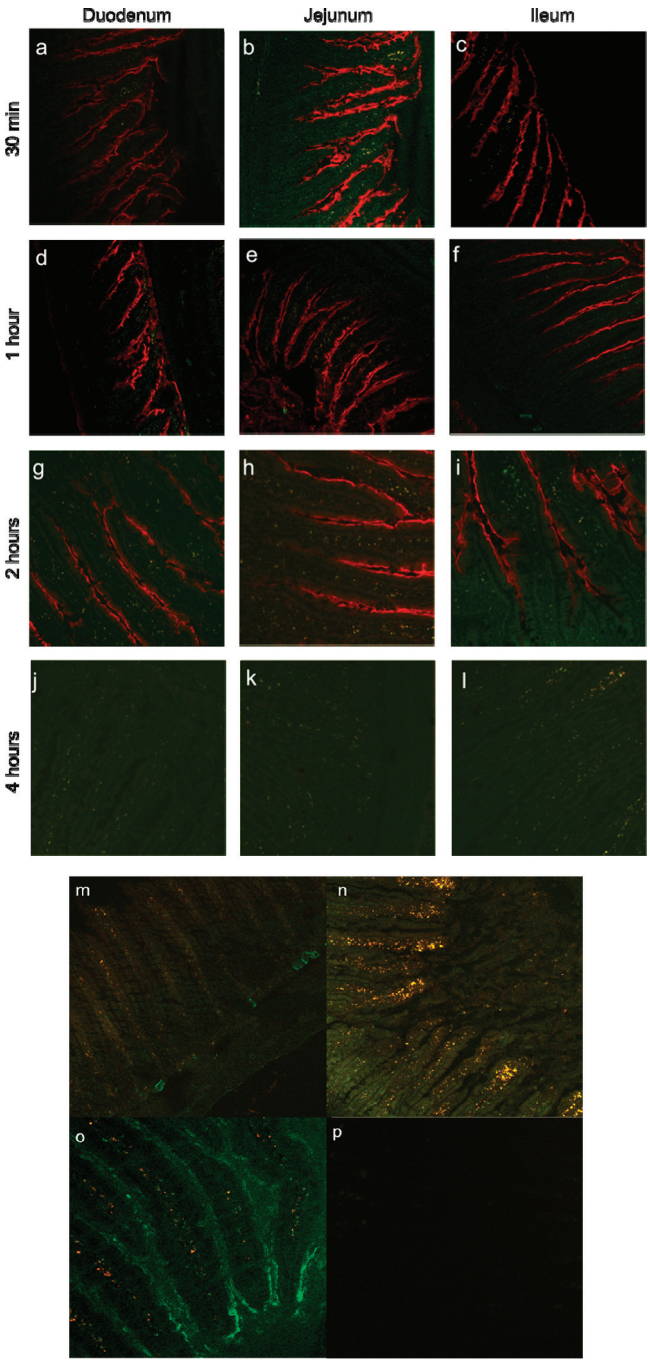

Figure 6. (a–l) Confocal laser scanning micrographs of rat intestinal tissue after dosing with GCPQ24–Texas Red (75 mg kg^{-1}). The Texas Red signal associates with the gastrointestinal mucosa and is not seen inside the cells of the villi. (m–p) Confocal laser scanning micrographs of rat small intestine 1 h after dosing with idarubicin (red/orange fluorescence) or GCPQ24–carboxyfluorescein (green fluorescence)–idarubicin. m = rat duodenum 1 h after dosing with idarubicin (10 mg kg^{-1}), n = rat duodenum 1 h after dosing with GCPQ24 (75 mg kg^{-1})–idarubicin (10 mg kg^{-1}) nanoparticles, o = rat jejunum 1 h after dosing with GCPQ24–carboxyfluorescein (75 mg kg^{-1})–idarubicin (10 mg kg^{-1}) nanoparticles, p = jejunum from control animal dosed with water. GCPQ24 is seen to associate with the intestinal mucus layer, and idarubicin is seen inside the villi having been absorbed.

TEER. The TEER is a measure of the permeability of the monolayer to ions, with a decrease in TEER indicating a permeability

dx.doi.org/10.1021/mp200469a | *Mol. Pharmaceutics* 2012, 9, 14–28

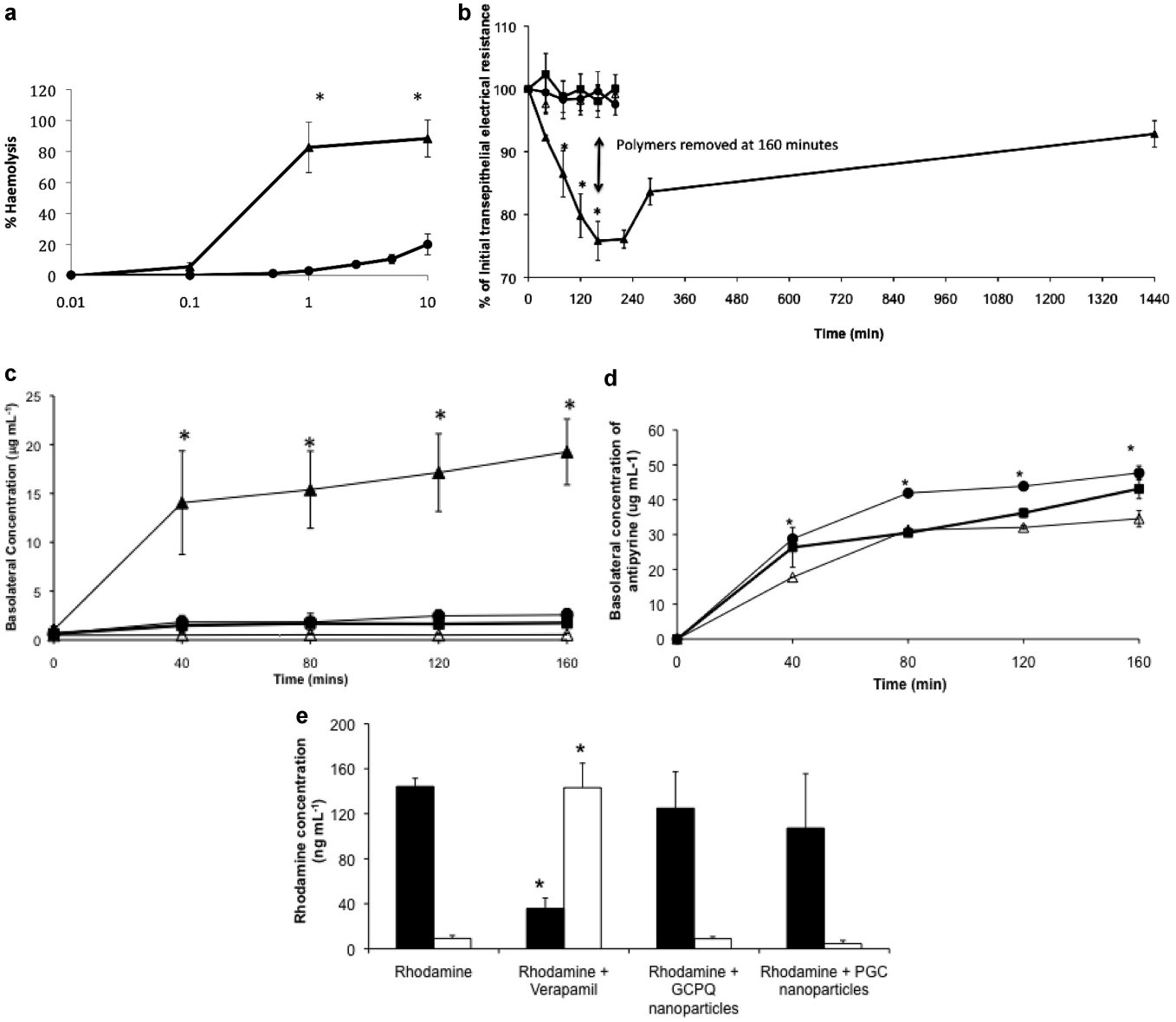

Figure 7. (a) The hemocompatibility of GCPQ24 nanoparticles: ● = GCPQ24 nanoparticles, ▲ = polysorbate 80; hemolysis caused by Triton-X 100 (10 mg mL^{-1} = 100% hemolysis while the hemolysis caused by phosphate buffered saline (pH = 7.4) = 0% hemolysis, * = significant differences ($p < 0.05$). (b) The effect of chitosan amphiphile nanoparticles on the transepithelial resistance across a Caco-2 cell monolayer: ■ = PGC24 nanoparticles (5 mg mL^{-1}), ● = GCPQ24 nanoparticles (5 mg mL^{-1}), ▲ = poly(ethylenimine) (0.4 μg mL^{-1}), Δ = Hanks buffered salt solution (pH = 7.4), * = significant differences ($p < 0.05$). (c) The apical to basolateral transport of Lucifer Yellow (0.5 mg mL^{-1}) across a Caco-2 cell monolayer: ■ = PGC24 nanoparticles (5 mg mL^{-1}), ● = GCPQ24 nanoparticles (5 mg mL^{-1}), ▲ = poly(ethylenimine) (0.4 μg mL^{-1}), Δ = Lucifer Yellow alone (0.5 mg mL^{-1}), * = significant differences between all polymers and Lucifer Yellow alone ($p < 0.05$). (d) The transport of antipyrine (0.4 mg mL^{-1}) across a Caco-2 monolayer: ■ = PGC24 nanoparticles (5 mg mL^{-1}), ● = GCPQ24 nanoparticles (5 mg mL^{-1}), Δ = antipyrine alone (0.4 mg mL^{-1}), * = significant differences ($p < 0.05$) between polymers and antipyrine alone; PGC24 is only significantly different from antipyrine alone at the 40, 120, and 160 min time points only; GCPQ24 is significantly different from PGC24 at the 80 and 120 min time points. (e) The effect of GCPQ24 and PGC24 on the P-glycoprotein efflux pump, rhodamine (1.9 μg mL^{-1}, 5 μM) was first placed in the apical compartment in the presence/absence of polymers/verapamil and the amount of rhodamine transported across to the basolateral compartment quantified after 90 min (white bars); in a separate experiment, rhodamine (1.9 μg mL^{-1}, 5 μM) was placed in the basolateral compartment, polymers and verapamil were placed in the apical compartment, and the amount of rhodamine transported to the apical compartment was quantified after 90 min (black bars), * = significant differences when compared to the transport of rhodamine alone, verapamil concentration = 49 μg mL^{-1} (0.1 mM), polymer concentrations = 1 mg mL^{-1}.

to ions and other hydrophilic solutes.[44] The TEER across the Caco-2 monolayers after 21 days was 300−500 Ω cm^{-2} and similar to values reported in the literature.[45] As expected, PEI 25kDa, the positive control known to significantly reduce TEER,[18] caused a 25% reduction in the TEER of the cell monolayers (Figure 7a). The effect was reversible in the long term. There was no reduction in the TEER observed with the chitosan amphiphile nanoparticles at the high concentration of 5 mg mL^{-1}.

Due to the formation of tight junctions by the Caco-2 cell monolayer, Lucifer Yellow, a paracellular marker, which is transported in between tight junctions, demonstrated very low

dx.doi.org/10.1021/mp200469a|*Mol. Pharmaceutics* 2012, 9, 14–28

permeability, with negligible amounts crossing the monolayer. The positive control, poly(ethylenimine), which increases the paracellular permeability across the Caco-2 cell monolayer, significantly increased (by over 20-fold) the amount of Lucifer Yellow transported across the monolayer from the apical to basolateral compartments (Figure 6b). The polymers GCPQ24 and PGC24 did cause a slight increase in the transport of Lucifer Yellow. However the amount of Lucifer Yellow transported across the monolayer in the presence of the chitosan amphiphiles was only 10% of that seen in the presence of poly(ethylenimine).

It is clear that the chitosan amphiphile nanoparticles do not appreciably alter the permeability of the monolayers to ions, or increase the paracellular permeability of the monolayer to any great extent, all indications that the nanoparticles do not open tight junctions. Chitosan in solution has been shown to open tight junctions[46] and produce a reduction in TEER across Caco-2 cell monolayers. We conclude the polymers in solution behave very differently from their aggregated amphiphilic analogues as although the cationic polymer—poly(ethylenimine) in solution opens tight junctions, the amphiphile cetyl quaternary ammonium poly(ethylenimine) does not open tight junctions.[18] It is speculated that the self-assembly of the amphiphile prevents the interaction of the polymer monomers (presumably polymer monomer cationic groups) with the appropriate tight junction proteins and in this way prevents the opening of tight junctions.

Antipyrine is a transcellular marker which passively diffuses across the Caco-2 monolayer with good permeability[47] and is also rapidly absorbed in the upper gastrointestinal tract.[48] When antipyrine alone was applied to the apical compartment of the Caco-2 cell monolayer, the concentration of antipyrine in the basolateral chamber reached a plateau after 80 min (Figure 7c) indicating that this was the maximum amount that can traverse the monolayer unaided. Both polymers significantly increased the transport of antipyrine resulting in a higher maximum plateau (Figure 7c). GCPQ24 was superior to PGC24 at enhancing the transcellular transport of antipyrine; GCPQ24 was statistically significantly superior to PGC24 at the 80 and 120 min time points. It is clear that both chitosan amphiphiles have a significant effect on the transcellular transport of antipyrine and that GCPQ24 is more effective at promoting transcellular transport than PGC24.

In order to examine if chitosan amphiphiles have any effect on the efflux transporters operating at the apical surface of the gastrointestinal epithelial cells, the effect of GCPQ24 on the transport of a known P-glycoprotein (P-gp) efflux pump substrate was measured. The P-gp efflux pump is one of the more extensively studied intestinal epithelium efflux transporters,[49] and rhodamine, a P-gp substrate,[50] was used to measure the effect of GCPQ24 on this transporter. The flux of rhodamine across the cell monolayer was assessed in both directions, the absorptive (apical to basolateral) and the secretory (basolateral to apical). When rhodamine was placed in the apical layer, the concentration of rhodamine transported to the basolateral compartment was low; however, when rhodamine was placed in the basolateral compartment, the concentration of rhodamine transported to the apical compartment was high (Figure 7d); both data sets indicate that rhodamine is actively transported out of the cell by transporters situated on the apical cell surface. In the presence of verapamil, a P-gp inhibitor,[35] in the apical compartment, the transport of rhodamine from the apical chamber to the basolateral chamber was high; while when rhodamine was placed in the basolateral chamber in the presence of verapamil in the apical chamber, the transport of rhodamine 123 to the apical chamber was low (Figure 7d), indicating that verapamil inhibited the secretory activity of the P-gp efflux pump. The presence of the polymers, however, did not alter the transport kinetics of rhodamine 123 and resulted in limited transport of rhodamine 123 from the apical to the basolateral chamber, an indication that these polymers do not inhibit the P-gp efflux pump.

DISCUSSION

We have previously shown that poly(ethylenimine) amphiphiles significantly enhance the absorption of hydrophobic actives such as cyclosporin A[18] by enhancing transcellular transport.[19] Here we present chitosan amphiphile polymer nanoparticles, which promote the absorption of both hydrophobic and hydrophilic drugs (Figure 5, Table 4). The mechanism of action, in the case of hydrophobic drugs, involves enhancing the dissolution of the drug from the nanoparticles (Figure 4j), bioadhesion of the nanoparticles to the functional aspects of the gastrointestinal tract (Figure 6) and the promotion of transcellular transport (Figure 7c) as depicted schematically in Figure 8. The

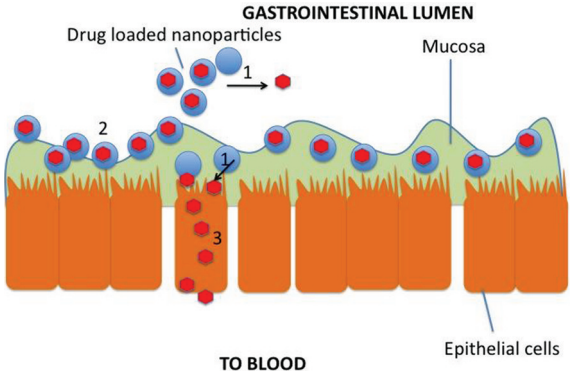

Figure 8. Chitosan amphiphile drug absorption enhancement proposed mechanism of action: 1 = accelerated dissolution from the high surface area nanoparticles; 2 = mucoadhesion to the absorptive regions of the upper gastrointestinal tract, prolonging drug residence time; 3 = transcellular transport of drug molecules across the gastrointestinal epithelium.

amphiphiles do not perturb intercellular tight junction permeability (Figure 7a,b) or inhibit the efflux activity of the P-glycoprotein efflux pump (Figure 7d). A clear nanoparticle contribution to the mechanism for the enhanced absorption of hydrophobic drugs thus emerges. First there is the stable (Figure 4i) encapsulation of the drug in nanoparticles with a high surface area (Figure 4c–h), from which drug dissolution is promoted (Figure 4i). The nanoparticles are extremely stable and maintain their payload for at least 6 months (Figure 4j). Polymer aggregation is usually driven by the entropy gain associated with the release of water molecules surrounding the hydrophobic cavity,[23,38,51] and the aggregation of PGC and GCPQ is entropy driven as indicated by a positive $T\Delta S$ of micellization. The stability of the nanoparticles stems from the entropy gain on micellization (Table 2), and this high entropy gain on micellization is due to the high apolar surface area (multiple C16 pendant groups) contained within each molecule as opposed to the poly(oxypropylene) block of the Pluronic block copolymers in which only the central methylene in the oxypropylene monomer is truly apolar. The net result is an extremely low CMC in the μM range (Table 2) as opposed to

the mM range seen with other polymeric amphiphiles (e.g., the Pluronics).[37] There is an influence of polymer molecular weight seen with the higher molecular weight drug−cyclosporin A (molecular weight = 1202 Da) as GCPQ24 is more efficient at enhanicng the oral absorption of cyclosporin A than GCPQ48 (Figure 5a). At the concentrations used, GCPQ24 encapsulates more cyclosporin A in the colloidal fraction of the formulation than GCPQ24 (Figure 4b). There is no polymer molecular weight effect seen with the lower molecular weight drug griseofulvin (molecular weight = 352 Da) (Figure 5b), despite the fact that there appears to be more drug in the colloidal fraction with the lower molecular weight polymer (Figure 4a). It is noted that the majority of griseofulvin is not encapsulated within the colloidal fraction of the formulation (Figure 4a). We conclude that higher molecular weight drugs require higher molecular weight polymers to ensure an enhancement in oral absorption and that this requirement is linked to the more efficient encapsulation of higher molecular weight drugs by the higher molecular weight polymers.

These stable nanoparticles are bioadhesive (Figure 6); hydrogels prepared from PGC have also been found to be bioadhesive.[52] This bioadhesive property confines the nanoparticles to the functional absorptive aspects of the upper gastrointestinal tract and retards their progress toward the colon, the net result of which is the production of a longer absorptive time window. The interaction of these particles with the mucus means that any released drug is in close proximity with the enterocytes and the hydrophobic drug payload, on exiting the nanoparticle, is less likely to precipitate in the normally extensive water barrier between the nanoparticle surface and the enterocytes. Additionally the nanoparticles are embedded in the mucosa and the mucosal barrier is circumvented. Any released drug thus is able to traverse the absorptive enterocytes via the transcellular route (Figure 7d) although the exact mechanism of this transcellular transport is still unclear but is the subject of a study in our laboratories. GCPQ is a more effective absorption enhancer than PGC (Figure 5) and promotes transcellular transport more efficiently than PGC (Figure 7c), an observation that supports the conclusion that an increase in transcellular transport underpins the mechanism of action of these polymer particles. It is not clear exactly why GCPQ is superior to PGC in promoting transcellular transport although we speculate that it could be linked to the higher encapsulation of drugs into smaller nanoparticles by the more hydrophilic GCPQ polymer (Figure 4a,b).

The mechanism of absorption enhancement for a hydrophilic drug such as ranitidine clearly does not involve the opening of tight junctions (Figure 7a,b). We know that PGC bilayer vesicles promote the cellular uptake of encapsulated hydrophilic macromolecules;[53] however, PGC is not an effective enhancer of hydrophilic drug absorption and GCPQ does not appear to be absorbed (Figure 6). It is possible that GCPQ particles embedded in the mucus layer would interact with the absorptive cells of the gastrointestinal tract and improve their permeability to (a) dissolved drug, (b) any drug associated with the nanoparticles, or (c) any drug also embedded in the mucosal layer.

■ ASSOCIATED CONTENT

Ⓢ Supporting Information

GPC−MALLS chromatograms, aggregation plots, and confocal laser scanning microscopy images. This material is available free of charge via the Internet at http://pubs.acs.org.

■ AUTHOR INFORMATION

Corresponding Author

*University of London, School of Pharmacy, Department of Pharmaceutics, 29−39 Brunswick Square, London, WC1N 1AX, U.K. Tel: +44 207 753 5997. Fax: +44 207 753 5942. E-mail: ijeoma.f.uchegbu@pharmacy.ac.uk.

■ REFERENCES

(1) Salama, N. N.; Eddington, N. D.; Fasano, A. Tight junction modulation and its relationship to drug delivery. *Adv. Drug Delivery Rev.* **2006**, *58* (1), 15−28.

(2) Davis, S. S. *Evaluation of the gastrointestinal transit and release characteristics of drugs*; Ellis Horwood Ltd.: Chichester, England, 1987.

(3) Aulton, M. E. *Pharmaceutics: The science of dosage form design*; Churchill: Livingston: 1992; p 734.

(4) Chillistone, S.; Hardman, J. Factors affecting drug absorption and distribution. *Pharmacology: Anaesthesia and Intensive Care Medicine* **2008**, *9* (4), 167−171.

(5) Kilpatrick, P. Pressures in the Pipeline. *Nat. Rev. Drug Discovery* **2003**, *2*, 337.

(6) Kesisoglou, F.; Panmai, S.; Wu, Y. Nanosizing - Oral formulation development and biopharmaceutical evaluation. *Adv. Drug Delivery Rev.* **2007**, *59*, 631−644.

(7) Stella, V. J.; Nti-Addae, K. W. Prodrug strategies to overcome poor water solubility. *Adv. Drug Delivery Rev.* **2007**, *59*, 677−694.

(8) Kilpatrick, P. Pressures in the pipeline. *Nat. Drug Discovery* **2003**, *2*, 337.

(9) Li, S.; Wong, S. M.; Sethia, S.; Almoazen, H.; Joshi, Y. M.; Serajuddin, A. T. M. Investigation of solubility and dissolution of a free base and two different salt forms as a function of pH. *Pharm. Res.* **2005**, *22*, 628−635.

(10) Burstein, A. H.; Cox, D. S.; Mistry, B.; Eddington, N. D. Phenytoin pharmacokinetics following oral administration of phenytoin suspension and fosphenytoin solution to rats. *Epilepsy Res.* **1999**, *34*, 129−133.

(11) Yagi, S.; Ono, J.; Yoshimoto, J.; Sugita, K. I.; Hattori, N.; Fujioka, T.; Fujuwara, T.; Sugimoto, H.; Hirano, K.; Hashimoto, N. Development of anti-influenza virus drugs I: improvement of oral absorption and in vivo anti-influenza activity of stachyflin and its derivatives. *Pharm. Res.* **1999**, *16*, 1041−1046.

(12) Tandya, A.; Dehghani, F.; Foster, N. R. Micronization of cyclosporine using dense gas techniques. *J. Supercrit. Fluids* **2006**, *37*, 272−278.

(13) Kayser, O.; Olbrich, C.; Yardley, V.; Kinderlen, A. F.; Croft, S. L. Formulation of amphotericin B as nanosuspensions for oral administration. *Int. J. Pharm.* **2003**, *254*, 73−75.

(14) Brewster, M. E.; Loftsson, T. Cyclodextrins as pharmaceutical solubilizers. *Adv. Drug Delivery Rev.* **2007**, *59*, 645−666.

(15) Szejtli, J. Past, present, and future of cyclodextrin research. *Pure Appl. Chem.* **2004**, *76*, 1825−1845.

(16) Wong, S. M.; Kellaway, I. W.; Murdan, S. Enhancement of the dissolution rate and oral absorption of a poorly water soluble drug by formation of surfactant-containing microparticles. *Int. J. Pharm.* **2006**, *317* (1), 61−68.

(17) Porter, C. J. H.; Trevaskis, N. L.; Charman, W. N. Lipids and lipid-based formulations: optimizing the oral delivery of lipophilic drugs. *Nat. Rev. Drug Discovery* **2007**, *6* (3), 231−248.

(18) Cheng, W. P.; Gray, A. I.; Tetley, L.; Hang, T. L. B.; Schatzlein, A. G.; Uchegbu, I. F. Polyelectrolyte nanoparticles with high drug loading enhance the oral uptake of hydrophobic compounds. *Biomacromolecules* **2006**, *7* (5), 1509−1520.

(19) Uchegbu, I. F.; Lane, M.; Schatzlein, A. G., Nanomedicines from polymeric amphiphiles. In *Handbook of Materials for Nanomedicines*; Torchilin, V. P., Amiji, M., Eds.; Pan Stanford Publishing: Singapore, 2010; pp 495−513.

(20) Lee, S.; Kim, S. K.; Lee, D. Y.; Park, K.; Kumar, T. S.; Chae, S. Y.; Byun, Y. Cationic analog of deoxycholate as an oral delivery carrier for ceftriaxone. *J. Pharm. Sci.* **2005**, *94* (11), 2541−2548.

(21) Qu, X. Z.; Khutoryanskiy, V. V.; Stewart, A.; Rahman, S.; Papahadjopoulos-Sternberg, B.; Dufes, C.; McCarthy, D.; Wilson, C. G.; Lyons, R.; Carter, K. C.; Schatzlein, A.; Uchegbu, I. F. Carbohydrate-based micelle clusters which enhance hydrophobic drug bioavailability by up to 1 order of magnitude. *Biomacromolecules* **2006**, *7* (12), 3452−3459.
(22) Qu, X.; Omar, L.; Le, T. B. H.; Tetley, L.; Bolton, K.; Chooi, K. W.; Wang, W.; Uchegbu, I. F. Polymeric amphiphile branching leads to rare nano-disc shaped planar self assemblies. *Langmuir* **2008**, *24*, 9997−10004.
(23) Chooi, K. W.; Gray, A. I.; Tetley, L.; Fan, Y. L.; Uchegbu, I. F. The molecular shape of poly(propylenimine) dendrimers has a profound effect on their self assembly. *Langmuir* **2010**, *26*, 2301−2316.
(24) Dwyer, C.; Viebke, C.; Meadows, J. Propofol induced micelle formation in aqueous block copolymer solutions. *Colloids Surf., A* **2005**, *254*, 23−30.
(25) Martin, L.; Wilson, C. G.; Koosha, F.; Tetley, L.; Gray, A. I.; Senel, S.; Uchegbu, I. F. The release of model macromolecules may be controlled by the hydrophobicity of palmitoyl glycol chitosan hydrogels. *J. Controlled Release* **2002**, *80* (1−3), 87−100.
(26) Lindenberg, M.; Kopp, S.; Dressman, J. B. Classification of orally administered drugs on the World Health Organization Model list of Essential Medicines according to the biopharmaceutics classification system. *Eur. J. Pharm. Biopharm.* **2004**, *58* (2), 265−278.
(27) Wang, W.; McConaghy, A. M.; Tetley, L.; Uchegbu, I. F. Controls on polymer molecular weight may be used to control the size of palmitoyl glycol chitosan polymeric vesicles. *Langmuir* **2001**, *17* (3), 631−636.
(28) Uchegbu, I. F.; Sadiq, L.; Arastoo, M.; Gray, A. I.; Wang, W.; Waigh, R. D.; Schätzlein, A. G. Quarternary ammonium palmitoyl glycol chitosan- a new polysoap for drug delivery. *Int. J. Pharm.* **2001**, *224*, 185−199.
(29) Wang, W.; Qu, X. Z.; Gray, A. I.; Tetley, L.; Uchegbu, I. F. Self-assembly of cetyl linear polyethylenimine to give micelles, vesicles, and dense nanoparticles. *Macromolecules* **2004**, *37* (24), 9114−9122.
(30) Kalyanasundaram, K.; Thomas, J. K. Environmental effects on vibrionic band intensities in pyrene monomer fluorescence and their application in studies of micellar systems. *J. Am. Chem. Soc.* **1977**, *99*, 2039−2044.
(31) Wang, G. J.; Engberts, J. Synthesis of Hydrophobically and Electrostatically Modified Polyacrylamides and Their Catalytic Effects on the Unimolecular Decarboxylation of 6-Nitrobenzisoxazole-3-Carboxylate Anion. *Langmuir* **1995**, *11* (10), 3856−3861.
(32) Molpeceres, J.; Guzman, M.; Bustamante, P.; Aberturas, M. Exothermic-endothermic heat of solution shift of cyclosporin A related to poloxamer 188 behaviour in aqueous solution. *Int. J. Pharm.* **1996**, *130*, 75−81.
(33) United States Pharmacopoeia Convention . *United States Pharmacopoeia*; United States Pharmacopoeia Convention: Rockville, MD, 2005.
(34) Walling, M. W.; Favus, M. J.; Kimberg, D. V. Effects of 25-Hydroxyvitamin D3 on Rat Duodenum, Jejunum, and Ileum − Correlation of Calcium Active Transport with Tissue Levels of Vitamin D_3 Metabolites. *J. Biol. Chem.* **1974**, *249*, 1156−1161.
(35) Hamilton, G.; Cosentini, E. P.; Teleky, B.; Koperna, T.; Zacheri, J.; Riegler, M.; Feil, W.; Schiessel, R.; Wenzi, E. The multidrug-resistance modifiers verapamil, cyclosporine-a and tamoxifen induce an intracellular acidification in colon-carcinoma cell-lines in-vitro. *Anticancer Res.* **1993**, *13* (6A), 2059−2063.
(36) Uchegbu, I. F.; Schatzlein, A. G.; Tetley, L.; Gray, A. I.; Sludden, J.; Siddique, S.; Mosha, E. Polymeric chitosan-based vesicles for drug delivery. *J. Pharm. Pharmacol.* **1998**, *50* (5), 453−8.
(37) Alexandridis, P.; Holzwarth, J. F.; Hatton, T. A. Micellization of Poly(Ethylene Oxide)-Poly(Propylene Oxide)- Poly(Ethylene Oxide) Triblock Copolymers in Aqueous-Solutions - Thermodynamics of Copolymer Association. *Macromolecules* **1994**, *27* (9), 2414−2425.
(38) Tanford, C. *The hydrophobic effect: formation of micelles and biological membranes*; John Wiley and Sons: New York, 1980.
(39) Chiu, Y. Y.; Higaki, K.; Neudeck, B. L.; Barnett, J. L.; Welage, L. S.; Amidon, G. L. Human jejunal permeability of cyclosporin A: Influence of surfactants on P-glycoprotein efflux in Caco-2 cells. *Pharm. Res.* **2003**, *20* (5), 749−756.
(40) Wagner, O.; Schreier, E.; Heitz, F.; Maurer, G. Tissue distribution, disposition, and metabolism of cyclosporine in rats. *Drug Metab. Dispos.* **1987**, *15*, 377−383.
(41) Takagi, T.; Ramachandran, C.; Bermejo, M.; Yamashita, S.; Yu, L. X.; Amidon, G. L. A provisional biopharmaceutical classification of the top 200 oral drug products in the United States, Great Britain, Spain, and Japan. *Mol. Pharmaceutics* **2006**, *3* (6), 631−643.
(42) Miller, R. Pharmacokinetics and bioavailability of ranitidine in humans. *J. Pharm. Sci.* **1984**, *73* (10), 1376−1379.
(43) GlaxoSmithKline. Zantac Prescribing Information. 2009, http://us.gsk.com/products/assets/us_zantac.pdf.
(44) Anderberg, E. K.; Artursson, P. Epithelial Transport Of Drugs In Cell-Culture 0.8. Effects Of Sodium Dodecyl-Sulfate On Cell-Membrane And Tight Junction Permeability In Human Intestinal Epithelial (Caco-2) Cells. *J. Pharm. Sci.* **1993**, *82* (4), 392−398.
(45) Dimitrijevic, D.; Lamandin, C.; Uchegbu, I. F.; Shaw, A. J.; Florence, A. T. The effect of monomers and of micellar and vesicular forms of non-ionic surfactants (Solulan C24 and Solulan 16) on Caco-2 cell monolayers. *J. Pharm. Pharmacol.* **1997**, *49* (6), 611−616.
(46) Artusson, P.; Lindmark, T.; Davis, S. S.; Illum, L. Effects of chitosan on the permeability of monolayers of intestinal epithelial cells (Caco-2). *Pharm. Res.* **1994**, *11*, 1358−1361.
(47) Lennernas, H.; Palm, K.; Fagerholm, U.; Artursson, P. Comparison between active and passive drug transport in human intestinal epithelial (Caco-2) cells in vitro and human jejunum in vivo. *Int. J. Pharm.* **1996**, *127* (1), 103−107.
(48) Masaoka, Y.; Tanaka, Y.; Kataoka, M.; Sakuma, S.; Yamashita, S. Site of drug absorption after oral administration: Assessment of membrane permeability and luminal concentration of drugs in each segment of gastrointestinal tract. *Eur. J. Pharm. Sci.* **2006**, *29* (3−4), 240−250.
(49) Hunter, J.; Hirst, B. H. Intestinal secretion of drugs. The role of P-glycoprotein and related drug efflux systems in limiting oral drug absorption. *Adv. Drug Delivery Rev.* **1997**, *25* (2−3), 129−157.
(50) Yumoto, R.; Murakami, T.; Nakamoto, Y.; Hasegawa, R.; Nagai, J.; Takano, M. Transport of rhodamine 123, a P-glycoprotein substrate, across rat intestine and Caco-2 cell monolayers in the presence of cytochrome P-450 3A-related compounds. *J. Pharmacol. Exp. Ther.* **1999**, *289* (1), 149−155.
(51) Gill, S. J.; Wadso, I. Equation of state describing hydrophobic interactions. *Proc. Natl. Acad. Sci. U.S.A.* **1976**, *73* (9), 2955−2958.
(52) Martin, L.; Wilson, C. G.; Koosha, F.; Uchegbu, I. F. Sustained buccal delivery of the hydrophobic drug denbufylline using physically cross-linked palmitoyl glycol chitosan hydrogels. *Eur. J. Pharm. Biopharm.* **2003**, *55*, 35−45.
(53) Dufes, C.; Schatzlein, A. G.; Tetley, L.; Gray, A. I.; Watson, D. G.; Olivier, J. C.; Couet, W.; Uchegbu, I. F. Niosomes and polymeric chitosan based vesicles bearing transferrin and glucose ligands for drug targeting. *Pharm. Res.* **2000**, *17* (10), 1250−1258.